

Unearthing the microbial ecology of soil carbon cycling with DNA-SIP

Charles Pepe-Ranney and Ashley N Campbell * †, Chantal Koechli †, Sean Berthrong, and Daniel H Buckley † ‡

* These authors contributed equally to the manuscript and should be considered co-first authors, † School of Integrative Plant Sciences, Cornell University, New York, USA, and ‡ corresponding author

Submitted to Proceedings of the National Academy of Sciences of the United States of America

Abstract

We explored the dynamics of microbial carbon (C) decomposition in soil by coupling DNA Stable Isotope Probing (SIP) and high throughput sequencing. Our experiment evaluated the degradative succession hypothesis, described dynamics of C metabolism during organic matter degradation, and characterized bacteria that metabolize labile and structural C in soils. We added a complex amendment representing plant derived organic matter to soil substituting ^{13}C -xylose or ^{13}C -cellulose for unlabeled equivalents in two experimental treatments. Xylose and cellulose are abundant components in plant biomass and represent labile and structural C pools, respectively. We assessed ^{13}C assimilation into DNA for SSU rRNA gene OTUs finding evidence of ^{13}C -incorporation from ^{13}C -xylose and ^{13}C -cellulose in 49 and 63 OTUs, respectively. Microorganisms primarily assimilated xylose-C into DNA on days 1, 3, and 7 and cellulose-C on days 14 and 30. The types of microorganisms that assimilated xylose-C changed with time dominated by *Firmicutes* at day 1 followed by *Bacteroidetes* at day 3 and then *Actinobacteria* at day 7. Temporal dynamics of ^{13}C -labeling suggests C traveled through different trophic levels within the soil bacterial community. Microbes that metabolized cellulose-C belonged to cosmopolitan soil lineages that remain uncharacterized physiologically including *Spartobacteria*, *Chloroflexi* and *Planctomycetes*. Our study links microorganisms to specific soil C processes revealing the ecological properties of specific microbial lineages and functionally defined groups of microbes within complex communities.

stable isotope probing | structure-function relationships | soil microbial ecology | 16S rRNA gene

Abbreviations: C, Carbon; OTU, Operational Taxonomic Unit; SOM, Soil Organic Matter; BD, Buoyancy Density; SIP, Stable Isotope Probing

Significance

Soil microorganisms drive C flux through the terrestrial biosphere, and intuitively, accounting for

microbial physiological diversity improves global C models. But, characterizing the ecophysiology of microbes involved with C decomposition in soil has proven difficult due to their overwhelming diversity. We characterized C use of microbial taxa in soil and show different C forms have distinct decomposition dynamics governed by different microbial lineages. For example, we found microbes belonging to uncharacterized but cosmopolitan taxa in soils assimilated cellulose-C into DNA. These microbes may drive cellulose decomposition on a global scale. We identify microbial lineages engaging in labile and structural C decomposition and explore their ecological properties.

Introduction

Soils worldwide contain 2,300 Pg of carbon (C) which accounts for nearly 80% of the C present in the terrestrial biosphere [1, 2]. C respiration by soil microorganisms produces annually tenfold more CO_2 than fossil fuel emissions [3]. Despite the contribution of microorganisms to global C flux, many global C models ignore the diversity of microbial physiology [4–6]. Further, predictions of climate change feedbacks on soil C flux improve when biogeochemical models explicitly represent microbial physiology [7]. However, we still know little about the ecophysiology of soil microorganisms, and such knowledge should assist the development and refinement of global C models [8–10]. Cellulose comprises most plant C (30–50%) followed by hemicellulose (20–40%), and lignin (15–25%) [11]. Hemicellulose, being the most soluble,

Reserved for Publication Footnotes

degrades in the early stages of decomposition. Xylans are often an abundant component of hemicellulose, and xylans themselves include differing amounts of xylose, glucose, arabinose, galactose, mannose, and rhamnose [12]. Xylose is often the most abundant sugar in hemicellulose, comprising as much as 60–90% of xylan in some plants (e.g. hardwoods) [13], wheat [14], and switchgrass [15]. Microbes that respire sugars proliferate during the initial stages of decomposition [16, 17], and metabolize as much as 75% of sugar C during the first 5 days of decomposition [18]. In contrast, cellulose decomposition proceeds more slowly with rates increasing for approximately 15 days and decomposition continues for 30–90 days [18, 19]. It is hypothesized that different microbial guilds mediate the decomposition of different plant biomass components [19–22]. The degradative succession hypothesis posits that fast growing organisms proliferate in response to the labile fraction of plant biomass such as sugars [23, 24] followed by slow growing organisms targeting structural C such as cellulose [23]. Evidence to support the degradative succession hypothesis comes from observing soil respiration dynamics and characterizing microbes cultured at different stages of decomposition. The degree to which the succession hypothesis presents an accurate model of litter decomposition has been questioned [21, 25, 26] and it's clear that we need new approaches to dissect microbial contributions to C transformations in soils.

Though microorganisms mediate 80–90% of the soil C-cycle [27, 28], and microbial community composition can account for significant variation in C mineralization [29], terrestrial C-cycle models rarely consider the community composition of soils [30, 31]. We measure rates of soil C transformations without knowledge of the organisms that mediate these reactions [28] leaving undefined the importance of community membership towards maintaining ecosystem function [28, 32, 33]. Variation in microbial community composition can be linked effectively to rates of soil processes when diagnostic genes for specific functions are available (e.g. denitrification [34], nitrification [35–37], methanotrophy [38], and nitrogen fixation [39]). However, the complexity of soil C transformations and the lack of diagnostic genes for describing these transformations has limited progress in characterizing the contributions of individual microbes to the soil C-cycle. Remarkably, we still lack basic information on the physiology and ecology of the majority of organisms that live in soils. For example, contributions to soil processes remain uncharacterized for entire and cosmopolitan bacterial phyla in soil such as *Acidobacteria*, *Chloroflexi*, *Planctomycetes*, and *Verrucomicrobia*. These phyla combined can

comprise 32% of soil microbial communities (based on surveys of the SSU rRNA genes in soil) [40, 41].

Characterizing the functions of microbial taxa has relied historically on culturing microorganisms and subsequently characterizing physiology in the laboratory, and on environmental surveys of genes diagnostic for specific processes. However, most microorganisms are difficult to grow in culture [40] and many processes lack suitable diagnostic genes. Nucleic acid stable-isotope probing (SIP) links genetic identity and activity without the need to grow microorganisms in culture and has expanded our knowledge of microbial contributions to biogeochemical processes [42]. However, nucleic acid SIP has notable complications including the need to add large amounts of labeled substrate [43], label dilution resulting in partial labeling of nucleic acids [43–45], the potential for cross-feeding and secondary label incorporation [45–50], and variation in genome G+C content [51–54]. As a result, most applications of SIP have targeted specialized microorganisms such as methanotrophs [43], methanogens [55], syntrophs [56], or microbes that target pollutants [57]. SIP has proved less useful for exploring the soil C-cycle because it has lacked the resolution necessary to pick up the complex signal that results from adding components of plant biomass to microbial communities in soil. High throughput DNA sequencing technology, however, improves the resolving power of SIP [58].

Coupling SIP with high throughput DNA sequencing now enables exploration of microbial C-cycling in soils. SSU rRNA amplicons can be sequenced from numerous density gradient fractions across multiple samples thereby increasing the resolution of a typical nucleic acid SIP experiment [59]. It is now possible to use far less isotopically labeled substrate resulting in more environmentally realistic experimental conditions [58]. We have employed such a high resolution DNA stable isotope probing approach to explore the assimilation of ¹³C labeled xylose and/or cellulose into bacterial DNA in an agricultural soil.

Specifically, we added to soil a complex amendment that simulated organic matter derived from fresh plant biomass. All treatments received the same amendment but the identity of isotopically labeled substrates was varied between treatments. We set up a control treatment where all components were unlabeled, a treatment with ¹³C-xylose instead of unlabeled xylose, and a treatment with ¹³C-cellulose instead of unlabeled cellulose. Soil was sampled at days 1, 3, 7, 14, and 30 and we identified which microorganisms assimilated ¹³C into DNA at each point in time. The experiment was designed to provide a test of the degradative succession hypothesis as it applies to soil bacteria, to identify soil bacteria that metabolize xylose and

cellulose, and to characterize temporal dynamics of xylose and cellulose metabolism in soil.

200 Results

After adding an organic matter amendment to soil, we tracked the flow of C from xylose or cellulose into microbial DNA over time using DNA-SIP (Figure S1). The amendment consisted of various plant biomass compounds including cellulose, lignin, sugars found in hemicellulose, amino acids, and inorganic salts (see Supplemental Information (SI)). The amendment was added at 2.3 mg C g⁻¹ soil dry weight (d.w.), and this comprised 16% of the total C in the soil. The cellulose-C (0.88 mg C g⁻¹ soil d.w.) and xylose-C (0.42 mg C g⁻¹ soil d.w.) in the amendment comprised 6% and 3% of the total C in the soil, respectively. The soil microbial community respiration 65% of the xylose within one day and 29% of the added xylose remained in the soil at day 30 (Figure S2). In contrast, cellulose-C declined at a constant rate of approximately 18 µg C d⁻¹ g⁻¹ soil d.w. and 40% of added cellulose-C remained in the soil at day 30 (Figure S2).

13C-labeling of OTUs changed with time and substrate. We assessed assimilation of ¹³C into microbial DNA by comparing the SSU rRNA gene sequence composition of SIP density gradient fractions between ¹³C treatments and controls (see Methods and SI). All treatments used the same amendment which included xylose and cellulose, but ¹³C-xylose or ¹³C-cellulose was substituted for its unlabeled equivalent in two amendments. A treatment without isotopically labeled components served as the control. In the gradient density fractions of the control treatment, fraction density represented the majority of the variance in SSU rRNA gene composition (Figure 1). DNA buoyant density correlates positively with G+C content [51] and therefore DNA G+C content influences variation in the SSU rRNA gene composition of density gradient fractions. For the ¹³C-cellulose treatment, SSU rRNA gene composition in gradient fractions deviated from control at high density (> 1.72 g mL⁻¹) on days 14 and 30 (Figure 1). For the ¹³C-xylose treatment, SSU rRNA gene composition in density gradient fractions also deviated from control in high density fractions, but in contrast to the ¹³C-cellulose treatment it deviated from control on days 1, 3, and 7 (Figure 1). SSU rRNA gene composition from ¹³C-cellulose treatment and ¹³C-xylose treatment density fractions differed at high density indicating different microorganisms assimilated C from xylose than cellulose (Figure 1). Further, in the ¹³C-cellulose treatment, the SSU rRNA gene sequence composition of high density

fractions at days 14 and 30 was similar indicating similar microorganisms had ¹³C-labeled DNA in ¹³C-cellulose treatments at days 14 and 30. In contrast, in the ¹³C-xylose treatment, the SSU rRNA gene composition of high density fractions varied between days 1, 3, and 7 indicating that different microbes had ¹³C-labeled DNA on these days. In the ¹³C-xylose treatment, the SSU gene composition of high density fractions was similar to control on days 14 and 30 (Figure 1) indicating that ¹³C was no longer detectable in bacterial DNA on these days for this treatment.

265 Temporal dynamics DNA ¹³C incorporation of OTUs. We monitored the soil microcosm microbial community over the course of the experiment by surveying SSU rRNA genes in non-fractionated DNA from the experimental soil. The SSU rRNA gene composition of the non-fractionated DNA changed with time (Figure S3, P-value = 0.023, R² = 0.63, Adonis test [60]). In contrast, the non-fractionated DNA SSU rRNA gene composition showed no statistical evidence for changing with treatment (P-value 0.23) (Figure S3). The latter result demonstrates the substitution of ¹³C-labeled substrates for unlabeled equivalents could not be shown to alter the soil microbial community composition. Twenty-nine OTUs exhibited sufficient statistical evidence (adjusted P-value < 0.10) to conclude they changed in relative abundance over the course of the experiment (Figure S4). When SSU rRNA gene abundances were combined at the taxonomic rank of “class”, the classes that changed in abundance (P-value < 0.10) were the *Bacilli* (decreased), *Flavobacteria* (decreased), *Gamma proteobacteria* (decreased), and *Herpetosiphonales* (increased) (Figure S5). Of the 29 OTUs that changed in relative abundance over time, 14 putatively incorporated ¹³C into DNA (Figure S4). OTUs that likely assimilated ¹³C from ¹³C-cellulose into DNA tended to increase in relative abundance with time whereas OTUs that assimilated ¹³C from ¹³C-xylose tended to decrease (Figure S6). OTUs that responded to both substrates did not exhibit a consistent relative abundance response over time as a group (Figure S4 and S6).

280 OTUs that assimilated ¹³C into DNA. If an OTU exhibited strong evidence for assimilating ¹³C into DNA, we refer to that OTU as a “responder” (see Methods for our operational definition of “responder”). The SSU rRNA gene sequences produced in this study were binned into 5,940 OTUs and we assessed evidence of ¹³C-labeling from both ¹³C-cellulose and ¹³C-xylose for each OTU. Forty-one OTUs responded to ¹³C-xylose, 55 OTUs responded to ¹³C-cellulose, and 8 OTUs responded

to both xylose and cellulose (Figure 2, Figure 3, 310 Figure S7, Table S1, and Table S2). The number of xylose responders peaked at days 1 and 3 and declined with time. In contrast, the number of cellulose responders increased with time peaking at 310 days 14 and 30 (Figure S8).

315 The phylogenetic composition of xylose responders changed with time and 86% of xylose responders shared > 97% SSU rRNA gene sequence identity with bacteria cultured in isolation (Figure 2 and 4). On day 1, *Bacilli* OTUs represented 320 84% of xylose responders and the majority of these OTUs were closely related to cultured representatives of the genus *Paenibacillus* (Table S1, Figure 3). For example, “OTU.57” (Table S1), annotated as *Paenibacillus*, had a strong signal of 325 ¹³C-labeling at day 1 coinciding with its maximum relative abundance in non-fractionated DNA. The relative abundance of “OTU.57” declined until day 14 and did not appear to be ¹³C-labeled after day 1 (Figure S9). On day 3, *Bacteroidetes* 330 OTUs comprised 63% of xylose responders (Figure 4) and these OTUs were closely related to cultured representatives of the *Flavobacteriales* and *Sphingobacteriales* (Table S1, Figure 3). For example, “OTU.14”, annotated as a flavobacterium, 335 had a strong signal for ¹³C-labeling in the ¹³C-xylose treatment at days 1 and 3 coinciding with its maximum relative abundance in non-fractionated DNA. The relative abundance of “OTU.14” then declined until day 14 and did not show evidence 340 of ¹³C-labeling beyond day 3 (Figure S9). Finally, on day 7, *Actinobacteria* OTUs represented 53% of the xylose responders and these OTUs were closely related to cultured representatives of *Micrococcales* (Table S1, Figure 3). For example, “OTU.4”, annotated as *Agromyces*, had signal for ¹³C-labeling 345 in the ¹³C-xylose treatment on days 1, 3 and 7 with the strongest evidence of ¹³C-labeling at day 7 and did not appear ¹³C-labeled at days 14 and 30. “OTU.4” relative abundance in non-fractionated 350 DNA increased until day 3 and then declined until day 30 (Figure S9). *Proteobacteria* were also common among xylose responders at day 7 where they comprised 40% of xylose responder OTUs. Notably, *Proteobacteria* represented the majority (6 355 of 8) of OTUs that responded to both cellulose and xylose (Figure S7).

The phylogenetic composition of cellulose responders did not change with time to the same extent as the xylose responders. Also, in contrast to xylose responders, cellulose responders often were not closely related (< 97% SSU rRNA gene sequence identity) to cultured isolates. Both the relative abundance and the number of cellulose responders increased over time peaking at 360 days 14 and 30 (Figure 2, Figure S8, and Figure S6). Cellulose responders belonged to the *Pro-*

teobacteria (46%), *Verrucomicrobia* (16%), *Planctomycetes* (16%), *Chloroflexi* (8%), *Bacteroidetes* (8%), *Actinobacteria* (3%), and *Melanobacteria* (1 OTU) (Table S2). The majority (86%) of cellulose responders in the *Proteobacteria* were closely related (> 97% identity) to bacteria cultured in isolation, including representatives of the genera: *Cellvibrio*, *Devosia*, *Rhizobium*, and *Sorangium*, which are all known for their ability to degrade cellulose (Table S2). Proteobacterial cellulose responders belonged to *Alpha* (13 OTUs), *Beta* (4 OTUs), *Gamma* (5 OTUs), and *Delta-proteobacteria* (6 OTUs).

The majority (85%) of cellulose responders outside of the *Proteobacteria* shared < 97% SSU rRNA gene sequence identity to bacteria cultured in isolation. For example, 70% of the *Verrucomicrobia* cellulose responders fell within unidentified *Spartobacteria* clades (Figure 3), and these shared < 85% SSU rRNA gene sequence identity to any characterized isolate. The *Spartobacteria* OTU “OTU.2192” exemplified many cellulose responders (Table S2, Figure S9). “OTU.2192” increased in non-fractionated DNA relative abundance with time and evidence for ¹³C-labeling of “OTU.2192” in the ¹³C-cellulose treatment increased over time with the strongest evidence at days 14 and 30 (Figure S9). Most *Chloroflexi* cellulose responders belonged to an unidentified clade within the *Herpetosiphonales* (Figure 3) and they shared < 89% SSU rRNA gene sequence identity to any characterized isolate. Characteristic of *Chloroflexi* cellulose responders, “OTU.64” increased in relative abundance over 30 days and evidence for ¹³C-labeling of “OTU.64” in the ¹³C-cellulose treatment peaked days 14 and 30 (Figure S9). Cellulose responders found within the *Bacteroidetes* fell within the *Cytophagales* in contrast with *Bacteroidetes* xylose responders that fell instead within the *Flavobacteriales* or *Sphingobacteriales* (Figure 3). *Bacteroidetes* cellulose responders included one OTU that shared 100% SSU rRNA gene sequence identity to species of *Sporocytophaga*, a genus that includes known cellulose degraders.

Characteristics of cellulose and xylose responders.

Cellulose responders, relative to xylose responders, tended to have lower relative abundance in non-fractionated DNA, demonstrated signal consistent with higher atom % ¹³C in labeled DNA, and had lower estimated *rrn* copy number (Figure 5). In the non-fractionated DNA, cellulose responders had lower relative abundance ($7e^{-4}$ (s.d. $2e^{-3}$)) than xylose responders ($2e^{-3}$ (s.d. $4e^{-3}$)) (Figure 4, P-value = 0.00028, Wilcoxon Rank Sum test). Six of the ten most common OTUs observed in the non-fractionated DNA responded to xylose,

and, eight of the ten most abundant responders
425 to xylose or cellulose in the non-fractionated DNA were xylose responders.

DNA buoyant density (BD) increases in proportion to the atom % ^{13}C of the DNA. Hence, the extent of ^{13}C incorporation into DNA can be evaluated by the difference in BD between ^{13}C -labeled and unlabeled DNA. We calculated for each OTU its mean BD weighted by relative abundance to determine its “center of mass” within a given density gradient. We then quantified for each OTU the difference in center of mass between control gradients and gradients from ^{13}C -xylose or ^{13}C -cellulose treatments (see SI for the detailed calculation). We refer to the change in center of mass position for an OTU in response to ^{13}C -labeling as $\Delta\hat{BD}$.
440 $\Delta\hat{BD}$ can be used to compare relative differences in ^{13}C -labeling between OTUs. $\Delta\hat{BD}$ values, however, are not comparable to the BD changes observed for DNA from pure cultures which generate molecules uniform in isotopic labeling, in part
445 because $\Delta\hat{BD}$ is based on relative abundance in density gradient fractions (and not DNA concentration) and in part because all members of an OTU may not respond uniformly to the isotopic label. Cellulose responder $\Delta\hat{BD}$ (0.0163 g mL^{-1}
450 (s.d. 0.0094)) was greater than that of xylose responders (0.0097 g mL^{-1} (s.d. 0.0094)) (Figure 5, P-value = 1.8610e^{-6} , Wilcoxon Rank Sum test).

We predicted the *rrn* gene copy number for responders as described [61]. The number of *rrn*
455 gene copies a microorganism has is correlated to its ability to proliferate after rapid nutrient influx [62]. Cellulose responders possessed fewer estimated *rrn* copy numbers (2.7 (1.2 s.d.)) than xylose responders (6.2 (3.4 s.d.)) (Figure 5 and Figure S10; P = 1.878e^{-9}). Furthermore, the estimated *rrn* gene copy number for xylose responders was inversely related to the day of first response (P = 2.02e^{-15} , Wilcoxon Rank Sum test, Figure S10, Figure 5).

460 We assessed phylogenetic clustering of ^{13}C -responsive OTUs with the Nearest Taxon Index (NTI) and the Net Relatedness Index (NRI) [63]. We also quantified the average clade depth of cellulose and xylose responders with the consenTRAIT metric [64]. Briefly, the NRI and NTI evaluate phylogenetic clustering against a null model for the distribution of a trait in a phylogeny. The NRI and NTI values are z-scores or standard deviations from the mean and thus the greater the magnitude of the NRI/NTI, the stronger the evidence for clustering (positive values) or overdispersion (negative values). NRI assesses overall clustering whereas the NTI assesses terminal clustering [65]. The consenTRAIT metric is a measure of the average clade depth for a trait in a phylogenetic tree. NRI values indicate that cellulose responders

clustered overall and at the tips of the phylogeny (NRI: 4.49, NTI: 1.43) while xylose responders clustered terminally (NRI: -1.33, NTI: 2.69). The consenTRAIT clade depth for xylose and cellulose responders was 0.012 and 0.028 SSU rRNA gene sequence dissimilarity, respectively. As reference, the average clade depth is approximately 0.017 SSU rRNA gene sequence dissimilarity for arabinose (another five C sugar found in hemicellulose) utilization as inferred from genomic analyses, and was 0.013 and 0.034 SSU rRNA gene sequence dissimilarity for glucosidase and cellulase genomic potential, respectively [64, 66]. These results indicate xylose responders form terminal clusters dispersed throughout the phylogeny while cellulose responders form deep clades of terminally clustered OTUs.
495

Discussion

500 We identified microorganisms participating in soil C cycling using a nucleic acid SIP approach. Specifically, we observed assimilation of ^{13}C from either ^{13}C -xylose or ^{13}C -cellulose into DNA for 104 OTUs in an agricultural soil. We found ^{13}C from 505 ^{13}C -xylose appeared to move into and then out of groups of related OTUs over time. By coupling nucleic acid SIP to high throughput sequencing we could diagnose OTU activity even when OTUs were at low relative abundance in non-fractionated DNA (e.g. on three occasions we did not detect 510 ^{13}C -responders in the non-fractionated DNA). Our results support the degradative succession hypothesis, elucidate ecophysiological properties of soil microorganisms, reveal activity of widespread uncultured soil bacteria, and begin to piece together the microbial food web in soils.

The degradative succession hypothesis predicts an ecological transition in activity during the decomposition of plant matter from microbes that 515 decompose labile plant biomass C to those that decompose structural more recalcitrant C. Our results concur with the degradative succession hypothesis. Microorganisms consumed xylose-C before cellulose-C and assimilated xylose-C into DNA faster than to cellulose-C. Xylose is major constituent of hemicellulose and is a labile component of fresh plant biomass. The phylogenetic composition of xylose responders changed between days 1, 3 and 7 and few OTUs appeared ^{13}C -labeled in the ^{13}C -xylose treatment after day 7. In the ^{13}C -cellulose treatment, few OTUs were ^{13}C -labeled in the beginning of the experiment but ^{13}C labeled OTUs increased at day 14 and maintained ^{13}C -labeling through day 30. Finally, 520 few (8 of 104) OTUs appeared to metabolize both xylose and cellulose meaning over 30 days cellulose responders succeeded xylose responders in activ-

ity. In addition to agreeing with the degradative succession hypothesis, our results suggest complex interactions between microbes occur during labile C decomposition.

Correlations between community composition and environmental characteristics often indirectly reveal microorganisms that belong to ecologically consistent groups [67]. In this experiment, we directly identified ecological groups as a function of *in situ* metabolism and inferred group ecological properties through phylogenetic affiliation, temporal dynamics of ^{13}C -assimilation, and the extent of ^{13}C -labeling per OTU. Xylose responders grew faster than cellulose responders and appeared to assimilate C from multiple sources. Xylose responders assimilated xylose-C into DNA within 24 hours and had low $\Delta\hat{BD}$ relative to cellulose responders suggesting xylose was not the sole C source used for growth. Xylose represented 20% of the amendment and 3.5% of total soil C. Xylose responders often included the most abundant OTUs within the non-fractionated DNA and had high estimated *rrn* copy number relative to cellulose responders. However, to some degree, high *rrn* gene copy number may inflate observed xylose responder relative abundance. Notably, the majority of xylose responder SSU rRNA genes (86%) matched SSU rRNA genes from cultured isolates at high sequence identity (> 97%).

Cellulose responders, on the other hand, incorporated ^{13}C into DNA after xylose responders and appeared to specialize in using cellulose as a C source. Cellulose responders grew over a span of weeks and had high $\Delta\hat{BD}$ indicating cellulose remained the dominant C source for cellulose responders even though multiple sources of C were present (cellulose represented 6% of total C present in soil at the start of the experiment). Cellulose responders were also lower in relative abundance on average within the non-fractionated DNA and had lower estimated *rrn* copy number than xylose responders. The majority of cellulose responders were not close relatives of cultured isolates although a number of cellulose responders shared high SSU rRNA gene sequence identity with cultured *Proteobacteria* (e.g. *Cellvibrio*). We identified cellulose responders among phyla such as *Verrucomicrobia*, *Chloroflexi*, and *Planctomycetes* – phyla whose functions within soil communities remain unknown.

Verrucomicrobia made up 16% of the cellulose responders. *Verrucomicrobia* are cosmopolitan soil microbes [68] that can make up to 23% of SSU rRNA gene sequences in soils [68] and 9.8% of soil SSU rRNA [69]. Genomic analyses and laboratory experiments show that various isolates within the *Verrucomicrobia* are capable of methanotrophy, diazotrophy, and cellulose degra-

dation [70, 71]. Moreover, *Verrucomicrobia* have been hypothesized to degrade polysaccharides in many environments [72–74]. However, only one of the 15 most abundant verrucomicrobial phylotypes in globally distributed soil samples shared > 93% SSU rRNA gene sequence identity with a cultured isolate [68] and hence the role of soil *Verrucomicrobia* in global C-cycling remains unknown. The majority of verrucomicrobial cellulose responders belonged to two clades that fall within the *Spartobacteria* (Figure 3). *Spartobacteria* outnumbered all other *Verrucomicrobia* phylotypes in SSU rRNA gene surveys of 181 globally distributed soil samples [68]. Given their ubiquity and abundance in soil as well as their demonstrated incorporation of ^{13}C from ^{13}C -cellulose, *Verrucomicrobia* lineages, particularly *Spartobacteria*, may be important contributors to cellulose decomposition on a global scale.

Other notable cellulose responders include OTUs in the *Planctomycetes* and *Chloroflexi* both of which have previously been shown to assimilate ^{13}C from ^{13}C -cellulose added to soil [75]. *Planctomycetes* are common in soil [40], comprising 4 to 7% of bacterial cells in many soils [76, 77] and 7% ± 5% of SSU rRNA [78]. Although soil *Planctomycetes* are widespread, their activities in soil remain uncharacterized. *Planctomycetes* represented 16% of cellulose responders and shared < 92% SSU rRNA gene sequence identity to their most closely related cultured isolates. *Chloroflexi* are known for metabolically dynamic lifestyles ranging from anoxygenic phototrophy to organohalide respiration [79] and are among the six most abundant bacterial phyla in soil [40]. Recent studies have focused on *Chloroflexi* roles in C cycling [79–81] and several *Chloroflexi* isolates use cellulose [79–81]. Four of the five *Chloroflexi* cellulose responders belong to a single clade within the *Herpetosiphonales* (Figure 3).

Finally, a single cellulose responder belonged to the *Melainabacteria* phylum (95% shared SSU rRNA gene sequence identity with *Vampirovibrio chlorellavorus*). The phylogenetic position of *Melainabacteria* is debated but *Melainabacteria* have been proposed to be a non-phototrophic sister phylum to *Cyanobacteria*. An analysis of a *Melainabacteria* genome [82] suggests the genomic capacity to degrade polysaccharides though *Vampirovibrio chlorellavorus* is an obligate predator of green alga [83]. The *Melainabacteria* cellulose responder did not respond to xylose so if it is predatory, it may prey specifically on structural C degraders (i.e. cellulose responders).

Responders did not necessarily assimilate ^{13}C into DNA directly from ^{13}C -xylose or ^{13}C -cellulose. In many ways, knowledge of secondary C degradation and/or microbial biomass turnover

may be more interesting with respect to the soil C-cycle than knowledge of primary degradation. The response to xylose suggests xylose-C moved through different trophic levels within the soil bacteria food web. The *Bacilli* degraded xylose first (65% of the xylose-C had been respired by day 1) representing 84% of day 1 xylose responders. *Bacilli* also comprised about 6% of SSU rRNA genes present in non-fractionated DNA on day 1. However, few *Bacilli* remained ¹³C-labeled by day 3 and their abundance declined reaching about 2% of soil SSU rRNA genes by day 30. Members of the *Bacillus* [84] and *Paenibacillus* in particular [59] have been previously implicated as labile C decomposers. The decline in relative abundance of *Bacilli* could be attributed to mortality and/or sporulation coupled to mother cell lysis. Concomitant with the decline in relative abundance and loss of ¹³C-label of *Bacilli*, *Bacteroidetes* OTUs appeared ¹³C-labeled at day 3. Finally, *Actinobacteria* appeared ¹³C-labeled at day 7 as *Bacteroidetes* xylose responders declined in relative abundance and became unlabeled. Hence, it seems reasonable to propose that *Bacteroidetes* and *Actinobacteria* xylose responders became ¹³C-labeled via the consumption ¹³C-labeled microbial biomass as opposed to primary degradation of ¹³C-xylose.

The inferred physiology of *Actinobacteria* and *Bacteroidetes* xylose responders provides further evidence that the activity dynamics represent C transfer between microbes by saprotrophy and/or predation. Most of the *Actinobacteria* xylose responders that appeared ¹³C-labeled at day 7 were members of the *Micrococcales* (Figure 3) and the most abundant ¹³C-labeled *Micrococcales* OTU at day 7 (OTU.4, Table S1) is annotated as belonging in the *Agromyces*. *Agromyces* are facultative predators that feed on the gram-positive *Luteobacter* in culture [85]. Additionally, certain types of *Bacteroidetes* can assimilate ¹³C from ¹³C-labeled *Escherichia coli* added to soil [86]. However, it is also possible that *Bacilli*, *Bacteroidetes*, and *Actinobacteria* are adapted to use xylose at different concentrations and that the observed activity dynamics resulted from changes in xylose concentration over time. If trophic transfer caused the activity dynamics, at least three different ecological groups exchanged C in 7 days. Models of the soil C cycle often exclude trophic interactions between soil bacteria (e.g. [87]), yet when soil C models do account for predators and/or saprophytes, trophic interactions are predicted to have significant effects on the fate of soil C [88].

Implications for soil C cycling models. Functional niche characterization for soil microorganisms is necessary to predict whether and how biogeochem-

ical processes vary with microbial community composition. Functional niches are defined by soil microbiologists and have been successfully incorporated into biogeochemical process models (E.g. [88, 89]). In some C models ecological strategies such as growth rate and substrate specificity are parameters for functional niche behavior [88]. The phylogenetic breadth of a functionally defined group is often inferred from the distribution of diagnostic genes across genomes [66] or from the physiology of isolates cultured on laboratory media [64]. For instance, the wide distribution of the glycolysis operon in microbial genomes is interpreted as evidence that many soil microorganisms participate in glucose turnover [10]. However, the functional niche may depend less on the distribution of diagnostic genes across genomes and more on life history traits that allow organisms to compete for a given substrate as it occurs in the soil. For instance, fast growth and rapid resuscitation allow microorganisms to compete for labile C which may often be transient in soil. Hence, life history traits may constrain the diversity of microbes that metabolize a given C source in the soil under a given set of conditions.

Biogeochemical processes mediated by a broad array of taxa are assumed to be less influenced by community change than narrow processes that involve a single, specific chemical transformation by a narrow suite of microbial participants [10, 90]. In addition, the diversity of a functionally defined group engaged in a specific C transformation is expected to correlate with C lability [10]. However, the diversity of active labile C and recalcitrant C decomposers in soil has not been directly quantified. We found comparable numbers of OTUs responded to ¹³C-cellulose and ¹³C-xylose (63 and 49, respectively). Cellulose responders were phylogenetically clustered suggesting that the ability to degrade cellulose is phylogenetically conserved. The clade depth of cellulose responders, 0.028 SSU rRNA gene sequence dissimilarity, is on the same order as that observed for glycoside hydrolases which are diagnostic enzymes for cellulose degradation [66]. Xylose responders clustered in terminal branches indicating groups of closely related taxa used xylose but xylose responders also clustered phylogenetically with respect to time of first response (Figure 3, Figure 4). For example, xylose responders on day 1 are dominated by members of *Paenibacillus*. Thus, microorganisms that degraded labile C and structural C were both limited in diversity. Although the genes for xylose metabolism are likely widespread in the soil community, it's possible limited groups of organisms had the ecological characteristics required to degrade xylose under the experimental conditions. Therefore it's possible few phylogenetically coherent

ent taxa actually participate in the metabolism
⁷⁷⁰ of labile C-sources under a given set of conditions, and hence changes in community composition may alter the dynamics of structural and labile C-transformations in soil.

Broadly, we observed labile C use by fast growing
⁷⁷⁵ generalists and structural C use by slow growing specialists. These results agree with the MIMICS model which simulates leaf litter decomposition by modeling microbial decomposers as two functionally defined groups, copiotrophs or oligotrophs [89]. Including these functional types improved predictions of C storage in response to environmental change relative to models that did not consider any microbial physiological diversity. We identified microbial lineages engaged in labile and structural C decomposition or simply, copiotrophs and oligotrophs. We also observed potentially greater turnover – and at the very least rate differences in turnover – for copiotroph biomass relative to oligotroph biomass which may be important to consider when modeling microbial turnover input to SOM. It's also clear that there may be more than two vital functional types mediating C-cycling in soil. That is, soil-C may travel through many bacterial trophic levels where each C transfer represents an opportunity for C stabilization in association with soil minerals or C loss by respiration.

Conclusion. Microorganisms sequester atmospheric C and respire SOM influencing climate change on a global scale but we do not know which microorganisms carry out specific soil C transformations. In this experiment microbes from physiologically uncharacterized but cosmopolitan soil lineages participated in cellulose decomposition. Cellulose responders included members of the *Verrucomicrobia* (*Spartobacteria*), *Chloroflexi*, *Bacteroidetes* and *Planctomycetes*. *Spartobacteria* in particular are globally cosmopolitan soil microorganisms and are often the most abundant *Verrucomicrobia* responder in soil [68]. Fast-growing aerobic spore formers from *Firmicutes* assimilated labile C in the form of xylose. Xylose responders within the *Bacteroidetes* and *Actinobacteria* likely became ¹³C-labeled by consuming ¹³C-labeled biomass that was labeled itself via the primary degradation of ¹³C-xylose. Our results suggest that cosmopolitan *Spartobacteria* may degrade cellulose on a global scale, labile plant biomass C may travel through a trophic cascade within the bacteria that includes predators and/or saprotrophs, and life history traits may act as a filter constraining the diversity of active microorganisms relative to those with the genomic potential for a given metabolism.

Methods

⁸²⁵ Additional information on sample collection and analytical methods is provided in Supplemental Materials and Methods.

Twelve soil cores (5 cm diameter x 10 cm depth) were collected from six sampling locations within ⁸³⁰ an organically managed agricultural field in Penn Yan, New York. Soils were sieved (2 mm), homogenized, distributed into flasks (10 g in each 250 ml flask, n = 36) and equilibrated for 2 weeks. We amended soils with a mixture containing 5.3 mg C ⁸³⁵ g⁻¹ soil dry weight (d.w.) and brought experimental soil to 50% water holding capacity. The amendment contained 38% cellulose, 23% lignin, 20% xylose, 3% arabinose, 1% galactose, 1% glucose, and 0.5% mannose by mass, with the remaining ⁸⁴⁰ 13.5% mass composed of an amino acid (in-house made replica of Teknova C0705) and macronutrient mixture (Murashige and Skoog, Sigma Aldrich M5524). This mixture approximates the molecular composition of switchgrass biomass with hemicellulose replaced by its constituent monomers [91]. We set up three parallel treatments varying the isotopically labeled component in each treatment. The treatments were (1) a control treatment with all unlabeled components, (2) a treatment with ⁸⁴⁵ ¹³C-cellulose instead of unlabeled cellulose (synthesized as described in SI), and (3) a treatment with ¹³C-xylose (98 atom% ¹³C, Sigma Aldrich) instead of unlabeled xylose. Other details relating to substrate addition can be found in Supplemental Methods. Microcosms were sampled destructively at days 1 (control and xylose only), 3, 7, 14, and 30 and soils were stored at -80°C until nucleic acid extraction. In the manuscript figures, the abbreviation 13CXPS refers to the ¹³C-xylose treatment ⁸⁵⁰ (¹³C Xylose Plant Simulant), 13CCPS refers to the ¹³C-cellulose treatment, and 12CCPS refers to the control treatment.

We used DESeq2 (R package), an RNA-Seq differential expression statistical framework [92], to ⁸⁵⁵ identify OTUs that were enriched in high density gradient fractions from ¹³C-treatments relative to corresponding density fractions from control treatments (for review of RNA-Seq differential expression statistics applied to microbiome OTU count data see (30)). We define “high density gradient fractions” as gradient fractions whose density falls between 1.7125 and 1.755 g ml⁻¹. Briefly, DESeq2 includes several features that enable robust estimates of standard error in addition to reliable ranking of logarithmic fold change (LFC) (i.e. gamma-Poisson regression coefficients) in relative abundance even with low count groups where LFC can often be noisy. Further, statistical evaluation of LFC can be performed with user-selected ⁸⁶⁰ thresholds as opposed to the often default null hypothesis that differential abundance for an OTU is

exactly zero enabling the most biologically interesting OTUs to be identified for subsequent analyses. We calculated LFC and corresponding standard errors for enrichment in ^{13}C treatments relative to control (high density fractions only) for each OTU. Subsequently, a one-sided Wald test was used to statistically assess LFC values (using corresponding standard errors). The user-defined null hypothesis for the Wald test was that LFC was less than one standard deviation above the mean of all LFC values. P-values were corrected for multiple comparisons using the Benjamini and Hochberg method [93]. We independently filtered OTUs on the basis of sparsity prior to correcting P-values for multiple comparisons. The sparsity value that yielded the most adjusted P-values less than 0.10 was selected for independent filtering by sparsity. Briefly, OTUs were eliminated if they failed to appear in at least 45% of high density gradient fractions for a given ^{13}C /control treatment pair. These sparse OTUs are unlikely to have sufficient data to allow for the determination of statistical significance. We selected a false discovery rate of 10% to denote statistical significance.

See Supplemental Information for DNA extraction, PCR, DNA sequence quality control, OTU ecological characteristic calculations, and SIP density gradient fractionation methods.

References

- Amundson R (2001) The carbon budget in soils. *Annu Rev Earth Planet Sci* 29(1): 535–562.
- Batjes N-H (1996) Total carbon and nitrogen in the soils of the world. *Eur J Soil Sci* 47(2): 151–163.
- Chapin F (2002) Principles of terrestrial ecosystem ecology. (Springer, New York)
- Allison S-D, Wallenstein M-D, Bradford M-A (2010) Soil-carbon response to warming dependent on microbial physiology. *Nat Geosci* 3(5): 336–340.
- Six J, Frey S-D, Thiet R-K, Batten K-M (2006) Bacterial and fungal contributions to carbon sequestration in agroecosystems. *Soil Sci Soc Am J* 70(2): 555.
- Treseder K-K, Balser T-C, Bradford M-A, Brodie E-L, Dumbinsky E-A, Eviner V-T, et al. (2011) Integrating microbial ecology into ecosystem models: challenges and priorities. *Biogeochemistry* 109(1–3): 7–18.
- Wieder W-R, Bonan G-B, Allison S-D (2013) Global soil carbon projections are improved by modelling microbial processes. *Nat Clim Chang* 3(10): 909–912.
- Bradford M-A, Fierer N, Reynolds J-F (2008) Soil carbon stocks in experimental mesocosms are dependent on the rate of labile carbon, nitrogen and phosphorus inputs to soils. *Funct Ecol* 22(6): 964–974.
- Neff J-C, Asner G-P (2001) Dissolved organic carbon in terrestrial ecosystems: synthesis and a model. *Ecosystems* 4(1): 29–48.
- McGuire K-L, Treseder K-K (2010) Microbial communities and their relevance for ecosystem models: Decomposition as a case study. *Soil Biol Biochem* 42(4): 529–535.
- Lynd L-R, Weimer P-J, van Zyl W-H, Pretorius I-S (2002) Microbial cellulose utilization: fundamentals and biotechnology. *Microbiology and molecular biology reviews* 66(3): 506–table of contents.
- Saha B-C (2003) Hemicellulose bioconversion. *J Ind Microbiol Biotechnol* 30(5): 279–291.
- Spiridon I, Popa V-I (2008) Chapter 13 - Hemicelluloses: Major Sources, Properties and Applications. *Monomers, Polymers and Composites from Renewable Resources*, , eds. Belgacem M-N, Gandini A (Elsevier, New York), pp 289–304.
- Sun X-F, Xu F, Zhao H, Sun R-C, Fowler P, Baird M-S (2005) Physicochemical characterisation of residual hemicelluloses isolated with cyanamide-activated hydrogen peroxide from organosolv pre-treated wheat straw. *Bioresour Technol* 96(12): 1342–1349.
- Bunnell K, Rich A, Luckett C, Wang Y-J, Martin E, Carrier D-J (2013) Plant maturity effects on the physicochemical properties and dilute acid hydrolysis of switchgrass (*Panicum virgatum*, l.) hemicelluloses. *ACS Sustain Chem Eng* 1(6): 649–654.
- Garrett S-D (1951) Ecological groups of soil fungi: a survey of substrate relationships. *New Phytol* 50(2): 149–166.
- Alexander M (1964) Biochemical ecology of soil microorganisms. *Annual Rev Microbiol* 18(1): 217–250.
- Engelking B, Flessa H, Joergensen R-G (2007) Microbial use of maize cellulose and sugarcane sucrose monitored by changes in the $^{13}\text{C}/^{12}\text{C}$ ratio. *Soil Biol Biochem* 39(8): 1888–1896.
- Hu S, van Bruggen A-H (1997) Microbial dynamics associated with multiphasic decomposition of ^{14}C -labeled cellulose in soil. *Microb Ecol* 33(2): 134–143.
- Rui J, Peng J, Lu Y (2009) Succession of bacterial populations during plant residue decomposition in rice field soil. *Appl Environ Microbiol* 75(14): 4879–4886.
- Kjöller A-H, Struwe S (2002) Fungal Communities, Succession, Enzymes, and Decomposition. *Enzymes in the Environment*, Books in Soils, Plants, and the Environment (Marcel Dekker, New York), pp 306–324.
- Bastian F, Bouziri L, Nicolardot B, Ranjard L (2009) Impact of wheat straw decomposition on successional patterns of soil microbial community structure. *Soil Biol Biochem* 41(2): 262–275.
- Garrett S-D (1963) Soil Fungi and soil fertility. (Pergamon Press, New York)
- Bremer E, Kuikman P (1994) Microbial utilization of $^{14}\text{C}[\text{U}]$ glucose in soil is affected by the amount and timing of glucose additions. *Soil Biol Biochem* 26(4): 511–517.
- Frankland J-C (1998) Fungal succession – unravelling the unpredictable. *Mycol Res* 102(1): 1–15.
- Osuno T (2005) Colonization and succession of fungi during decomposition of Swida controversa leaf litter. *Mycologia* 97(3): 589–597.
- Coleman D-C, Crossley D-A (1996) Fundamentals of soil ecology. (Academic Press, Waltham, Massachusetts)
- Nannipieri P, Ascher J, Ceccherini M-T, Landi L, Pietramellara G, Renella G (2003) Microbial diversity and soil functions. *Eur J Soil Sci* 54(4): 655–670.
- Strickland M-S, Lauber C, Fierer N, Bradford M-A (2009) Testing the functional significance of microbial community composition. *Ecology* 90(2): 441–451.
- Zak D-R, Blackwood C-B, Waldrup M-P (2006) A molecular dawn for biogeochemistry. *Trends Ecol Evol* 21(6): 288–295.
- Reed H-E, Martiny J-BH (2007) Testing the functional significance of microbial composition in natural communities. *FEBS Microbiol Ecol* 62(2): 161–170.
- Schimel J-P, Schaeffer S-M (2012) Microbial control over carbon cycling in soil. *Front Microbiol* 3: 348. doi: 10.3389/fmicb.2012.00348
- Allison S-D, Martiny J-BH (2008) Resistance resilience, and redundancy in microbial communities. *Proc Natl Acad Sci USA* 105(Supplement 1): 11512–11519.
- Cavigelli M-A, Robertson G-P (2000) The functional significance of denitrifier community composition in a terrestrial ecosystem. *Ecology* 81(5): 1402–1414.
- Carney K-M, Matson P-A, Bohannan B-JM (2004) Diversity and composition of tropical soil nitrifiers across a plant diversity gradient and among land-use types. *Ecol Lett* 7(8): 684–694.
- Hawkes C-V, Wren I-F, Herman D-J, Firestone M-K (2005) Plant invasion alters nitrogen cycling by modifying the soil nitrifying community. *Ecol Lett* 8(9): 976–985.
- Webster G, Embley T-M, Freitag T-E, Smith Z, Prosser J-I (2005) Links between ammonia oxidizer species composition, functional diversity and nitrification kinetics in grassland soils. *Environ Microbiol* 7(5): 676–684.
- Gulledge J, Doyle A-P, Schimel J-P (1997) Different NH_4^+ -inhibition patterns of soil CH_4 consumption: A result of distinct CH_4 -oxidizer populations across sites? *Soil Biol Biochem* 29(1): 13–21.
- Hsu S-F, Buckley D-H (2009) Evidence for the functional significance of diazotroph community structure in soil. *ISME J* 3(1): 124–136.

40. Janssen P-H (2006) Identifying the dominant soil bacterial
1035 taxa in libraries of 16S rRNA and 16S rRNA genes. *Appl Environ Microbiol* 72(3): 1719–1728.
41. Buckley D-H, Schmidt T-M (2002) Exploring the diversity
of soil - a microbial rainforest. *Biodiversity of Microbial Life: Foundation of Earth's Biosphere*, , ed. Reysenbach A-L (Wiley, New York, New York, USA), pp 183–208.
- 1040 42. Chen Y, Murrell J-C (2010) When metagenomics meets stable-isotope probing: progress and perspectives. *Trends Microbiol* 18(4): 157–163.
43. Radajewski S, Ineson P, Parekh N-R, Murrell J-C (2000)
1045 Stable-isotope probing as a tool in microbial ecology. *Nature* 403(6770): 646–649.
44. Manefield M, Whitley A-S, Griffiths R-I, Bailey M-J (2002) RNA Stable isotope probing: a novel means of linking microbial community function to phylogeny. *Appl Environ Microbiol* 68(11): 5367–5373.
- 1050 45. McDonald I-R, Radajewski S, Murrell J-C (2005) Stable isotope probing of nucleic acids in methanotrophs and methylotrophs: A review. *Org Geochem* 36(5): 779–787.
46. Morris S-A, Radajewski S, Willison T-W, Murrell J-C (2002) Identification of the functionally active methanotroph population in a peat soil microcosm by stable-isotope probing. *Appl Environ Microbiol* 68(3): 1446–1453.
- 1055 47. Hutchens E, Radajewski S, Dumont M-G, McDonald I-R, Murrell J-C (2004) Analysis of methanotrophic bacteria in Movie Cave by stable isotope probing. *Environ Microbiol* 6(2): 111–120.
48. Lueders T, Manefield M, Friedrich M (2004) Enhanced sensitivity of DNA- and rRNA-based stable isotope probing by fractionation and quantitative analysis of isopycnic centrifugation gradients. *Environ Microbiol* 6: 73–8.
- 1060 49. DeRito C-M, Pumphrey G-M, Madsen E-L (2005) Use of field-based stable isotope probing to identify adapted populations and track carbon flow through a phenol-degrading soil microbial community. *Appl Environ Microbiol* 71(12): 7858–7865.
50. Ziegler S-E, White P-M, Wolf D-C, Thoma G-J (2005)
1065 Tracking the fate and recycling of ¹³C-labeled glucose in soil. *Soil Sci* 170(10): 767–778.
51. Buckley D-H, Huangyutitham V, Hsu S-F, Nelson T-A (2007) Stable isotope probing with ¹⁵N achieved by disentangling the effects of genome G+C content and isotope enrichment on DNA density. *Appl Environ Microbiol* 73(10): 3189–3195.
- 1070 52. Birnie G-D (1978) Centrifugal separations in Molecular and cell biology. (Butterworth & Co Publishers Ltd, Boston)
53. Holben W-E, Harris D (1995) DNA-based monitoring of total bacterial community structure in environmental samples. *Molecular Ecology* 4(5): 627–632.
- 1075 54. Nüsslein K, Tiedje J-M (1999) Soil bacterial community shift correlated with change from forest to pasture vegetation in a tropical soil. *Appl Environ Microbiol* 65(8): 3622–3626.
55. Lu Y, Conrad R (2005) In situ stable isotope probing of methanogenic archaea in the rice rhizosphere. *Science* 309(5737): 1088–1090.
- 1080 56. Lueders T, Pommernke B, Friedrich M-W (2004) Stable-isotope probing of microorganisms thriving at thermodynamic limits: syntrophic propionate oxidation in flooded soil. *Appl Environ Microbiol* 70(10): 5778–5786.
57. DeRito C-M, Pumphrey G-M, Madsen E-L (2005) Use of field-based stable isotope probing to identify adapted populations and track carbon flow through a phenol-degrading soil microbial community. *Appl Environ Microbiol* 71(12): 7858–7865.
- 1085 58. Aoyagi T, Hanada S, Itoh H, Sato Y, Ogata A, Friedrich M-W, et al. (2015) Ultra-high-sensitivity stable-isotope probing of rRNA by high-throughput sequencing of isopycnic centrifugation gradients. *Environ Microbiol Rep* 7(2): 282–287.
59. Verastegui Y, Cheng J, Engel K, Kolczynski D, Mortimer S, Lavigne J, et al. (2014) Multisubstrate isotope labeling and metagenomic analysis of active soil bacterial communities. *mBio* 5(4): e01157–14.
- 1090 60. Anderson M-J (2001) A new method for non-parametric multivariate analysis of variance. *Austral Ecol* 26(1): 32–46.
61. Kembel S-W, Wu M, Eisen J-A, Green J-L (2012) Incorporating 16S gene copy number information improves estimates of microbial diversity and abundance. *PLoS Comput Biol* 8(10): e1002743.
62. Klappenbach J-A, Dunbar J-M, Schmidt T-M (2000) rRNA Operon copy number reflects ecological strategies of bacteria. *Appl Environ Microbiol* 66(4): 1328–1333.
63. Webb C-O (2000) Exploring the phylogenetic structure of ecological communities: an example for rain forest trees. *Am Nat* 156(2): 145–155.
- 1095 64. Martiny A-C, Treseder K, Pusch G (2013) Phylogenetic conservatism of functional traits in microorganisms. *ISME J* 7(4): 830–838.
65. Evans S-E, Wallenstein M-D (2014) Climate change alters ecological strategies of soil bacteria. *Ecol Lett* 17(2): 155–164.
66. Berlemont R, Martiny A-C (2013) Phylogenetic distribution of potential cellulases in bacteria. *Appl Environ Microbiol* 79(5): 1545–1554.
67. Fierer N, Bradford M-A, Jackson R-B (2007) Toward an ecological classification of soil bacteria. *Ecology* 88(6): 1354–1364.
68. Bergmann G-T, Bates S-T, Eilers K-G, Lauber C-L, Caporaso J-G, Walters W-A, et al. (2011) The under-recognized dominance of Verrucomicrobia in soil bacterial communities. *Soil Biol Biochem* 43(7): 1450–1455.
69. Buckley D-H, Schmidt T-M (2001) Environmental factors influencing the distribution of rRNA from Verrucomicrobia in soil. *FEMS Microbiol Ecol* 35(1): 105–112.
70. Wertz J-T, Kim E, Breznak J-A, Schmidt T-M, Rodrigues J-LM (2011) Genomic and physiological characterization of the Verrucomicrobia isolate *diplosphaera colitermitum* gen. nov. sp. nov., reveals microaerophily and nitrogen fixation genes. *Appl Environ Microbiol* 78(5): 1544–1555.
71. Otsuka S, Ueda H, Suenaga T, Uchino Y, Hamada M, Yokota A, et al. (2012) *Roseimicrobium gellanolyticum* gen. nov. sp. nov., a new member of the class Verrucomicrobiae. *Int J Syst Evol Microbiol* 63(Pt 6): 1982–1986.
72. Fierer N, Ladau J, Clemente J-C, Leff J-W, Owens S-M, Pollard K-S, et al. (2013) Reconstructing the microbial diversity and function of pre-agricultural tallgrass prairie soils in the united states. *Science* 342(6158): 621–624.
73. Chin K-J, Hahn D, Hengstmann U, Liesack W, Janssen P-H (1999) Characterization and identification of numerically abundant culturable bacteria from the anoxic bulk soil of rice paddy microcosms. *Appl Environ Microbiol* 65(11): 5042–5049.
74. Herlemann D-PR, Lundin D, Labrenz M, Jurgens K, Zheng Z, Asperg H, et al. (2013) Metagenomic de novo assembly of an aquatic representative of the verrucomicrobial class spartobacteria. *mBio* 4(3): e0056912.
75. Schellenberger S, Kolb S, Drake H-L (2010) Metabolic responses of novel cellulolytic and saccharolytic agricultural soil Bacteria to oxygen. *Environ Microbiol* 12(4): 845–861.
76. Zarda B, Hahn D, Chatzinotas A, Schnhuber W, Neef A, Amann R-I, et al. (1997) Analysis of bacterial community structure in bulk soil by *in situ* hybridization. *Arch Microbiol* 168(3): 185–192.
77. Chatzinotas A, Sandaa R-A, Schnhuber W, Amann R, Daee F-L, Torsvall V, et al. (1998) Analysis of broad-scale differences in microbial community composition of two pristine forest soils. *Syst Appl Microbiol* 21(4): 579–587.
78. Buckley D-H, Schmidt T-M (2003) Diversity and dynamics of microbial communities in soils from agro-ecosystems. *Environ Microbiol* 5(6): 441–452.
79. Hug L-A, Castelle C-J, Wrighton K-C, Thomas B-C, Sharon I, Frischkorn K-R, et al. (2013) Community genomic analyses constrain the distribution of metabolic traits across the Chloroflexi phylum and indicate roles in sediment carbon cycling. *Microbiome* 1(1): 22.
80. Goldfarb K-C, Karaouz U, Hanson C-A, Santee C-A, Bradford M-A, Treseder K-K, et al. (2011) Differential growth responses of soil bacterial taxa to carbon substrates of varying chemical recalcitrance. *Front Microbiol* 2: 94. doi: 10.3389/fmicb.2011.00094
81. Cole J-K, Gieler B-A, Heisler D-L, Palisoc M-M, Williams A-J, Dohnalkova A-C, et al. (2013) *Kallotenuis papyrolyticum* gen. nov. sp. nov., a cellulolytic and filamentous thermophile that represents a novel lineage (Kallotenuales ord. nov., Kallotenuaceae fam. nov.) within the class Chloroflexia. *Int J Syst Evol Microbiol* 63(Pt 12): 4675–4682.
82. Rienzi S-CD, Sharon I, Wrighton K-C, Koren O, Hug L-A, Thomas B-C, et al. (2013) The human gut and groundwater harbor non-photosynthetic bacteria belonging to a new candidate phylum sibling to Cyanobacteria. *eLIFE* 2: e01102.



83. Gromov B-V, Mamkaeva K-A (1972) [Electron microscopic study of parasitism by Bdellovibrio chlorellavorus bacteria on cells of the green alga Chlorella vulgaris]. *Tsitologiya* 14(2): 256–260.
- 1200 84. Cleveland C-C, Nemergut D-R, Schmidt S-K, Townsend A-R (2007) Increases in soil respiration following labile carbon additions linked to rapid shifts in soil microbial community composition. *Biogeochemistry* 82(3): 229–240.
- 1205 85. Casida L-E (1983) Interaction of *Agromyces ramosus* with other bacteria in soil. *Appl Environ Microbiol* 46(4): 881–888.
- 1210 86. Lueders T, Kindler R, Miltner A, Friedrich M-W, Kaestner M (2006) Identification of bacterial micropredators distinctively active in a soil microbial food web. *Appl Environ Microbiol* 72(8): 5342–5348.
- 1215 87. Moore J-C, Walter D-E, Hunt H-W (1988) Arthropod regulation of micro- and mesobiota in below-ground detrital food webs. *Annu Rev Entomol* 33(1): 419–435.
88. Kaiser C, Franklin O, Dieckmann U, Richter A (2014) Microbial community dynamics alleviated stoichiometric constraints during litter decay. *Ecol Lett* 17(6): 680–690.
89. Wieder W-R, Grandy A-S, Kallenbach C-M, Bonan G-B (2014) Integrating microbial physiology and physiochemical principles in soils with the MiCrobial-MIneral Carbon Stabilization (MIMICS) model. *Biogeosciences* 11(14): 3899–3917.
90. Schimel J (1995) Ecosystem consequences of microbial diversity and community structure. *Arctic and alpine biodiversity: patterns, causes and ecosystem consequences*, eds. Chapin III F-S, Körner C, Ecological Studies (Springer, Berlin Heidelberg), pp 239–254.
91. Schneckenberger K, Demin D, Stahr K, Kuzyakov Y (2008) Microbial utilization and mineralization of ^{14}C glucose added in six orders of concentration to soil. *Soil Biol Biochem* 40(8): 1981–1988.
92. Love M-I, Huber W, Anders S (2014) Moderated estimation of fold change and dispersion for RNA-seq data with DESeq2. *Genome Biol* 15(12): 550.
93. Benjamini Y, Hochberg Y (1995) Controlling the false discovery rate: A practical and powerful approach to multiple testing. *Journal of the Royal Statistical Society. Series B (Methodological)* 57(1): 289–300.

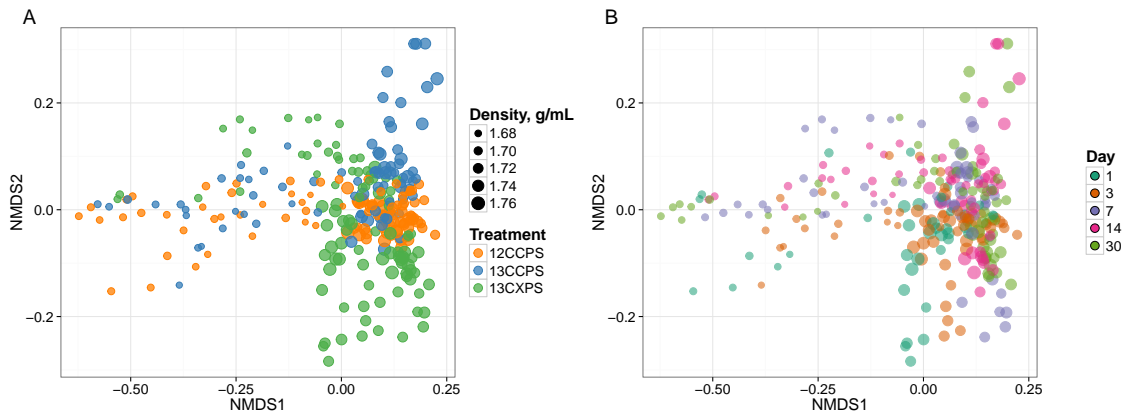


Fig. 1. NMDS analysis from weighted unifrac distances of 454 sequence data from SIP fractions of each treatment over time. Twenty fractions from a CsCl gradient fractionation for each treatment at each time point were sequenced (Fig. S1). Each point on the NMDS represents the bacterial composition based on 16S sequencing for a single fraction where the size of the point is representative of the density of that fraction and the colors represent the treatments (A) or days (B).

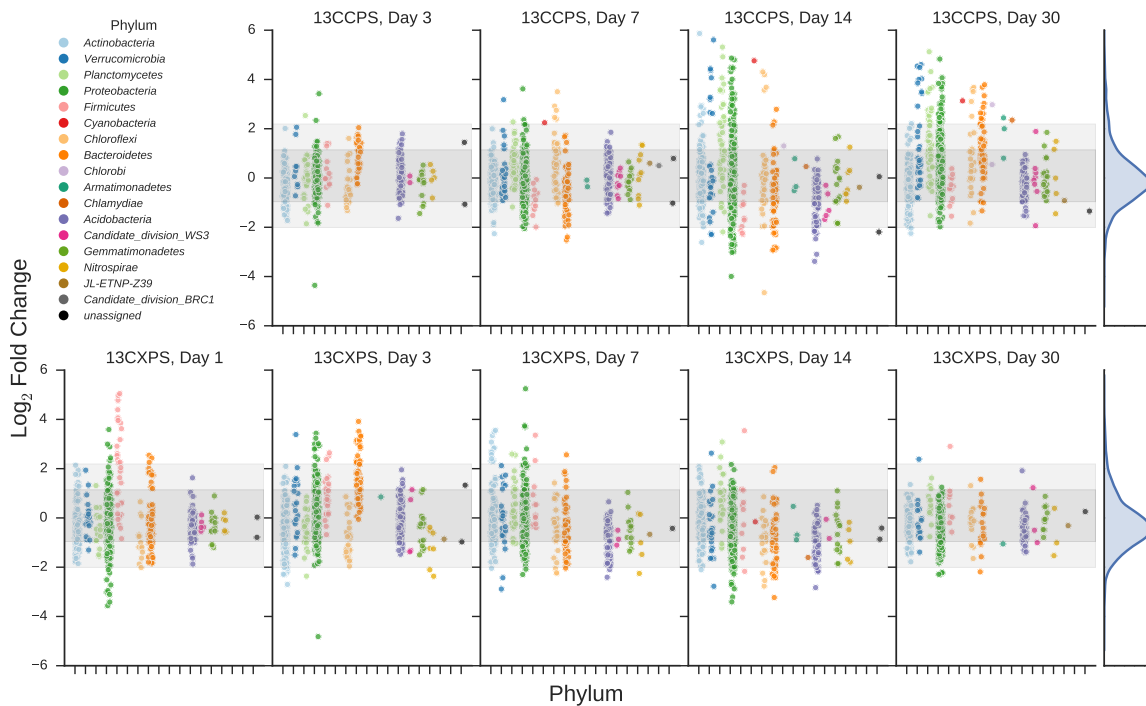


Fig. 2. Log₂ fold change of ¹³C-responders in cellulose treatment (top) and xylose treatment (bottom). Log₂ fold change is based on the relative abundance in the experimental treatment compared to the control within the density range 1.7125–1.755 g ml⁻¹. Taxa are colored by phylum. The last column shows the distribution of all fold change values in each row. The darker gray band represents one standard deviation and the lighter band represents two standard deviations about the mean of all fold change values for both treatments.

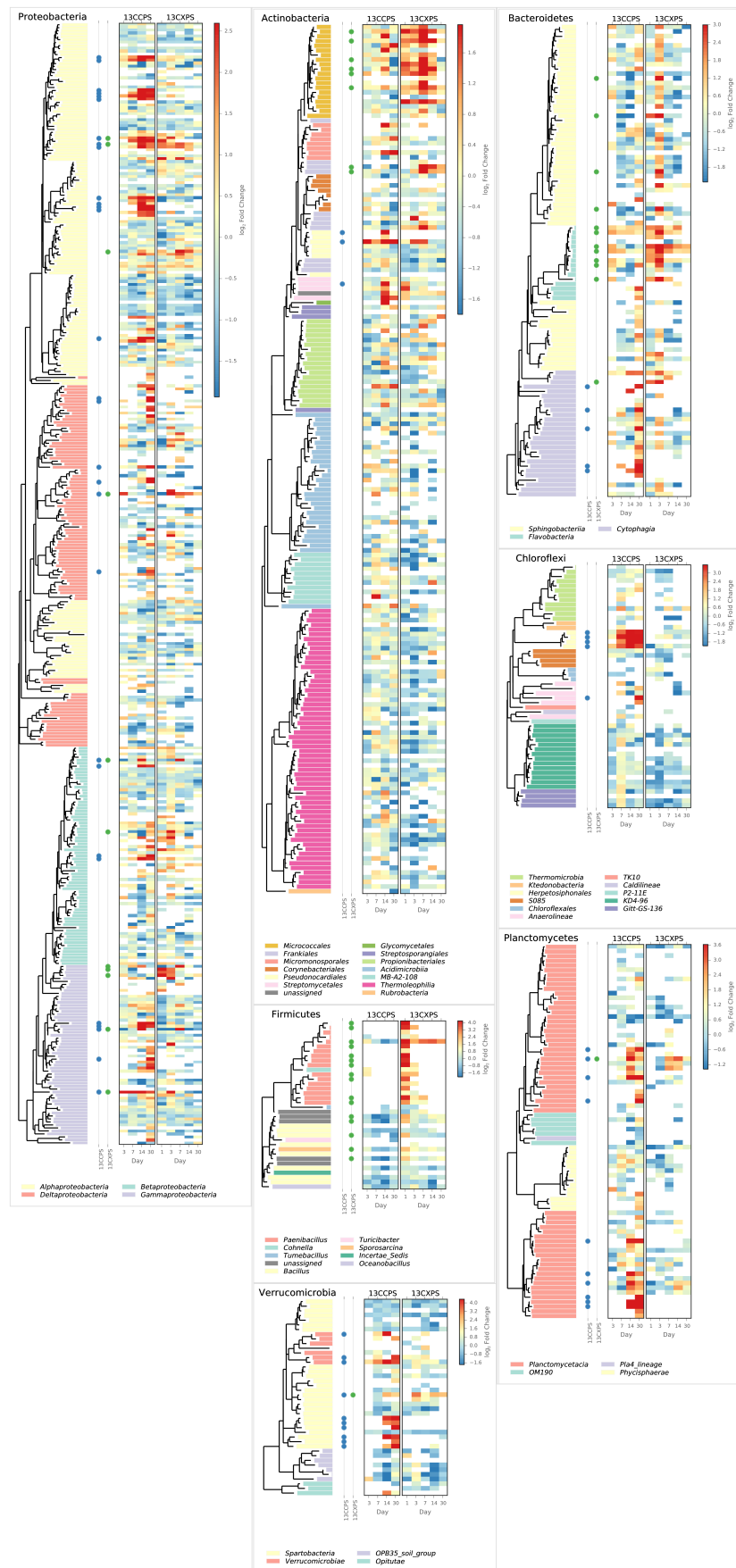


Fig. 3. Phylum specific trees. Heatmap indicates fold change between heavy fractions of control gradients versus labeled gradients. Dots indicate the position of "responders" to ^{13}C -xylose (green) or ^{13}C -cellulose (blue).

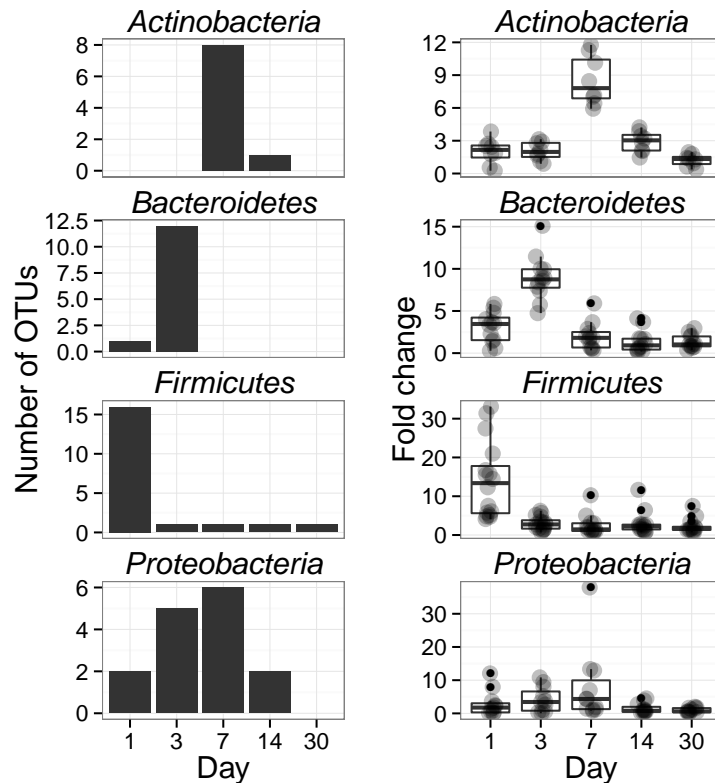


Fig. 4. Left column shows counts of ^{13}C -xylose responders in the *Actinobacteria*, *Bacteroidetes*, *Firmicutes* and *Proteobacteria* at days 1, 3, 7 and 30. Right panel shows OTU fold enrichment in heavy gradient fractions for ^{13}C -xylose amendment DNA relative to corresponding control fractions.

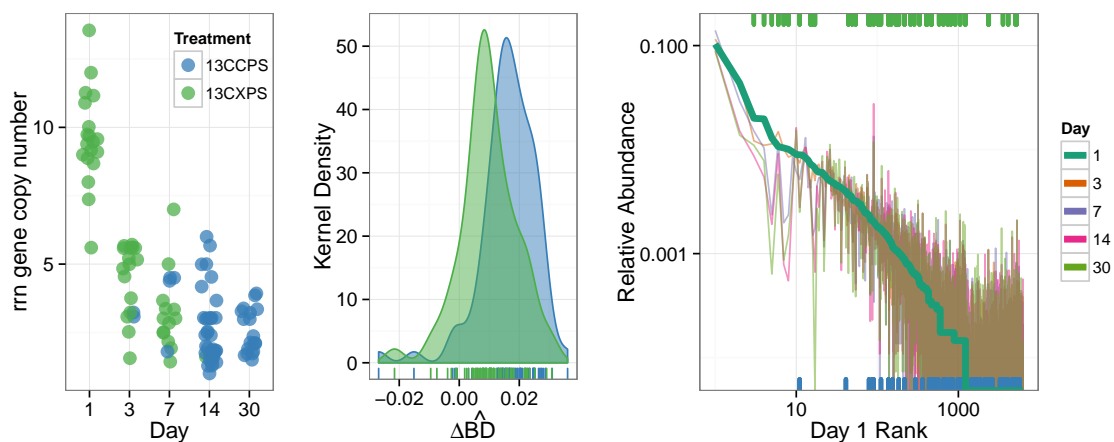


Fig. 5. ^{13}C -responder characteristics based on density shift (A) and rank (B). Kernel density estimation of ^{13}C -responder's density shift in cellulose treatment (blue) and xylose treatment (green) demonstrates degree of labeling for responders for each respective substrate. ^{13}C -responders in rank abundance are labeled by substrate (cellulose, blue; xylose, green). Ticks at top indicate location of ^{13}C -cylose responders in bulk community. Ticks at bottom indicate location of ^{13}C -cellulose responders in bulk community. OTU rank was assessed from day 1 bulk samples.

1240 **Supplemental Figures and Tables**

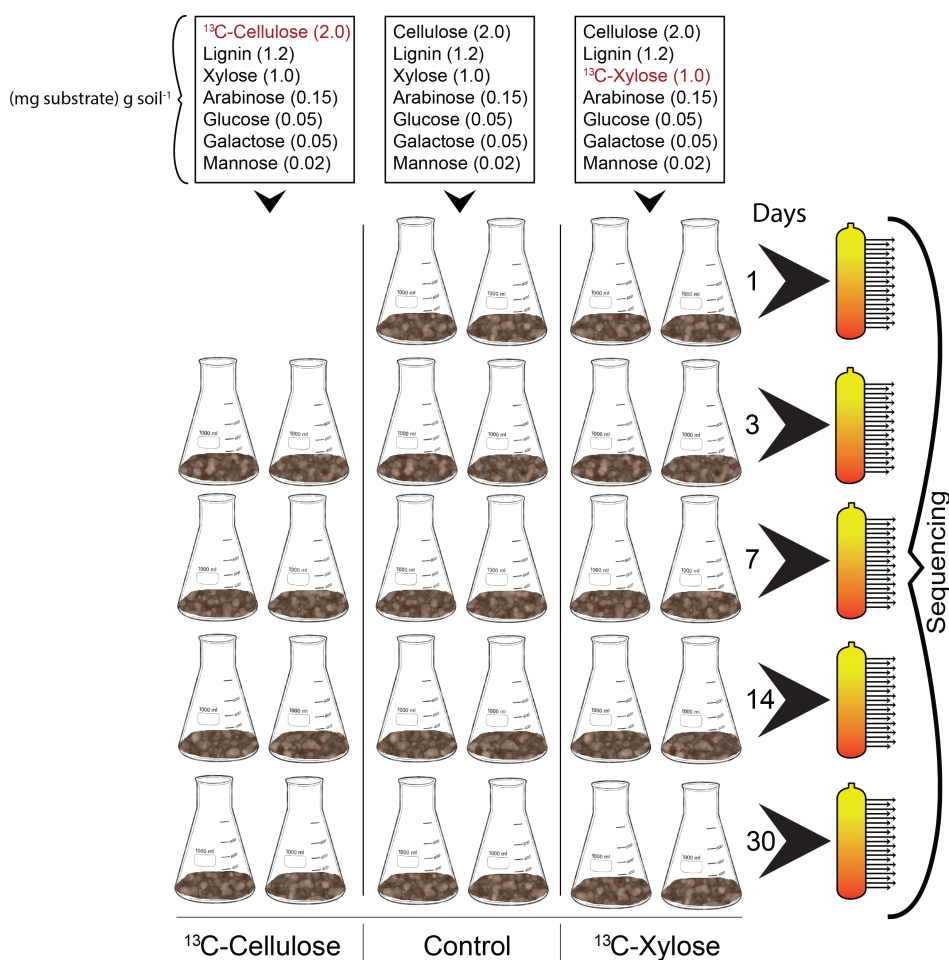


Fig. S1. The experimental design. A carbon mixture, in addition to inorganic salts and amino acids (not shown here), was added to each soil microcosm where the only difference between treatments is the ¹³C-labeled isotope (in red). At days 1, 3, 7, 14, and 30 replicate microcosms were destructively harvested for downstream molecular applications. Bulk DNA from each treatment and time point ($n = 14$) was CsCl density separated by centrifuged and fractionated (orange tubes wherein each arrow represents a fraction from the density gradient). Fractions were 16S gene sequenced using next generation sequencing technology.

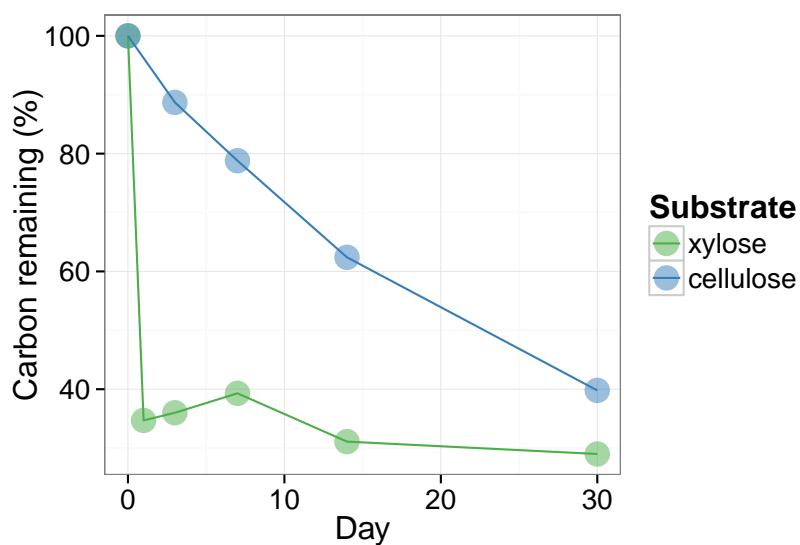
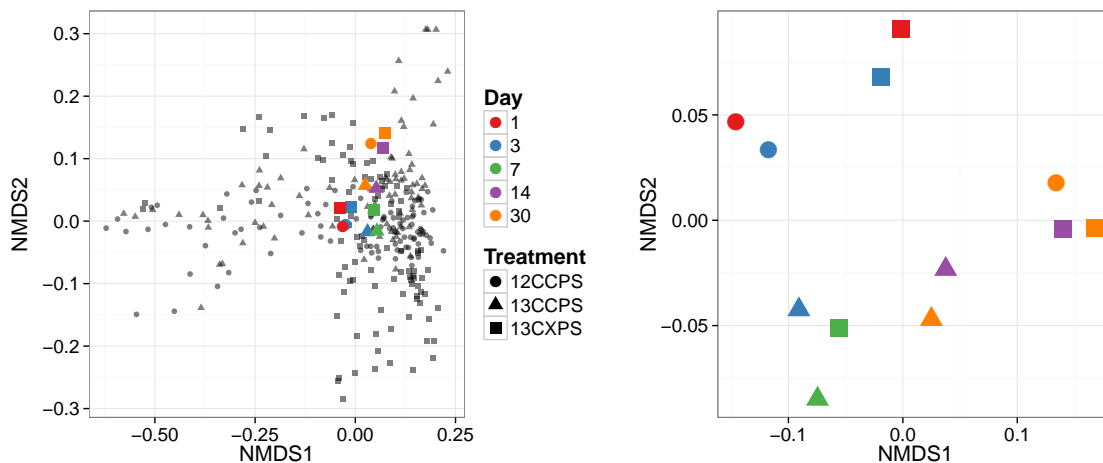
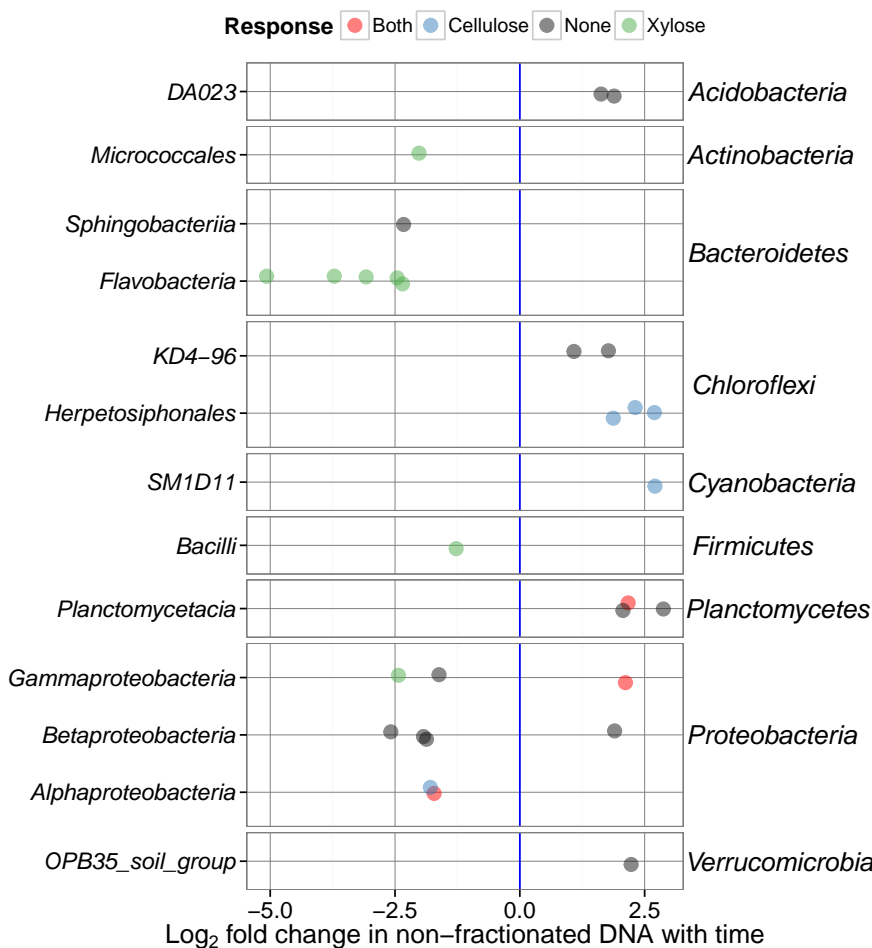


Fig. S2. Percentage of added ¹³C remaining in soil over time.

**Fig. S3.** Ordination of bulk gradient fraction phylogenetic profiles.**Fig. S4.** Fold change time⁻¹ for OTUs that changed significantly in abundance over time. One panel per phylum (phyla indicated on the right). Taxonomic class indicated on the left.

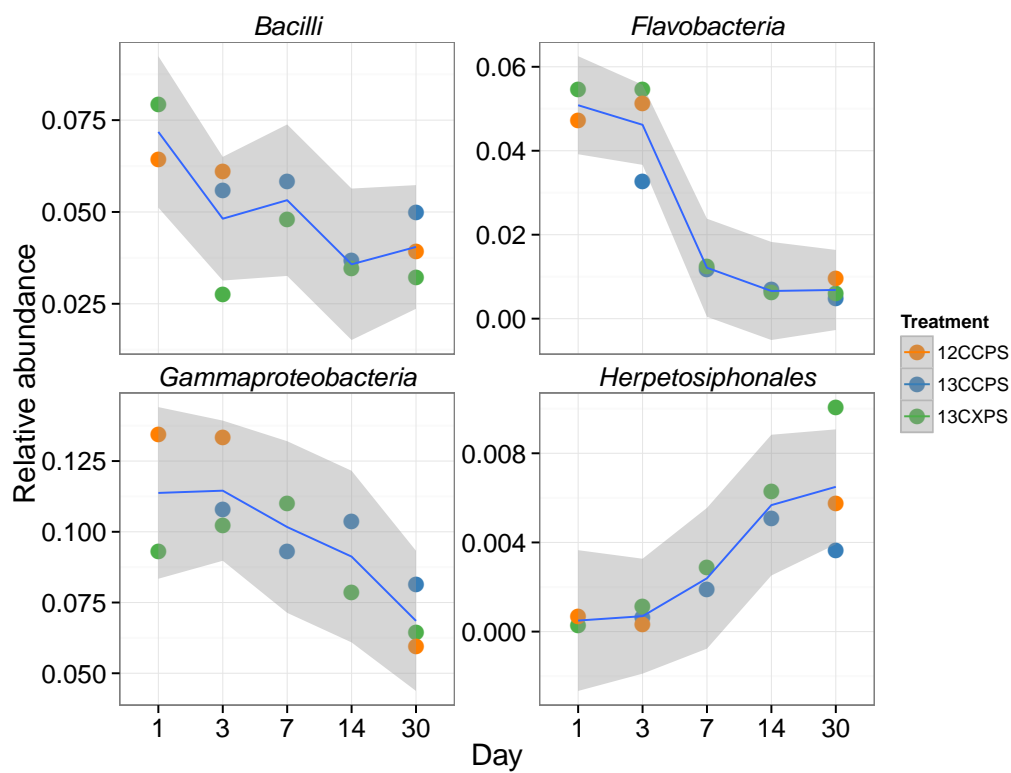
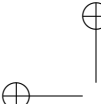
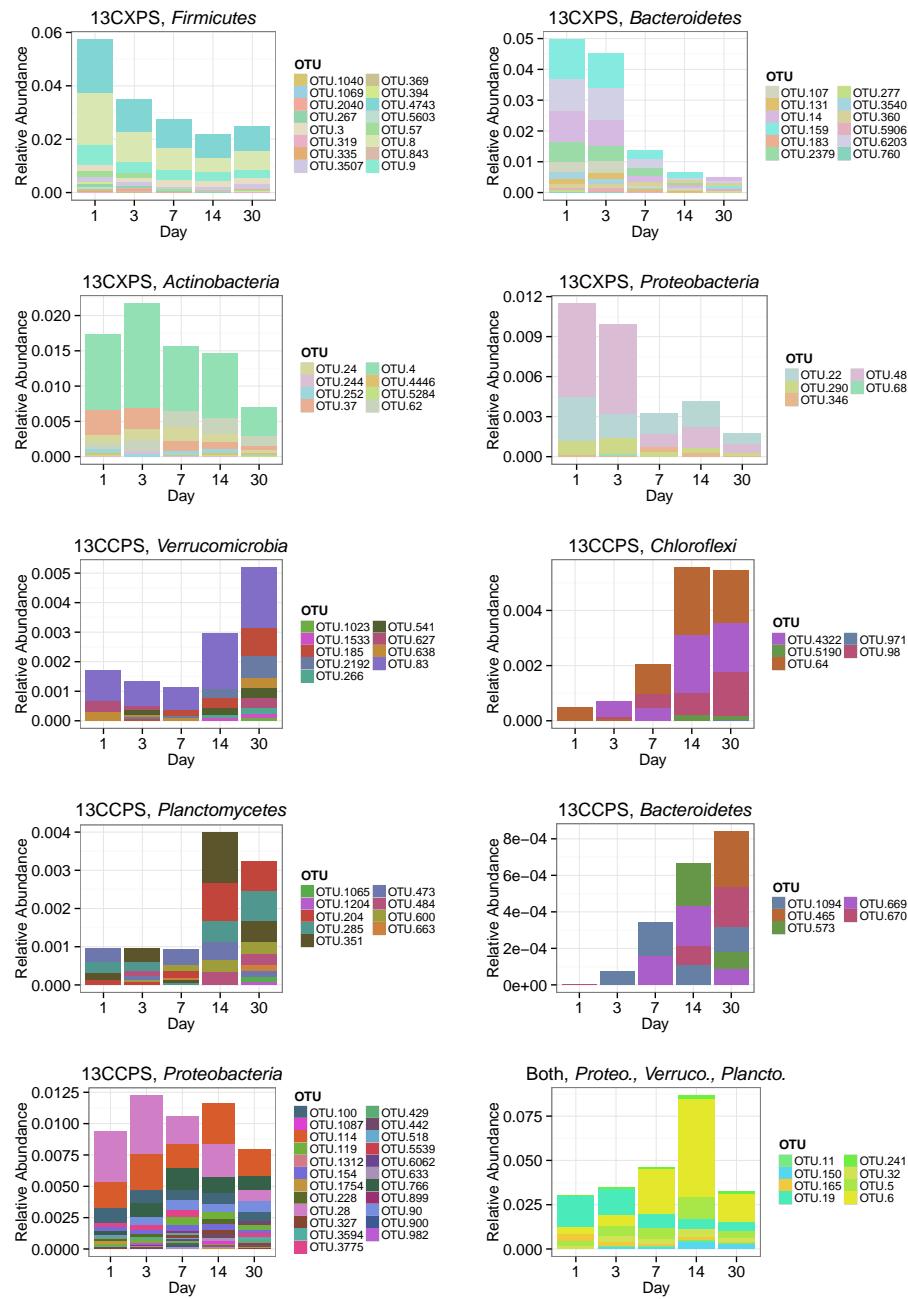


Fig. S5. Relative abundance versus day for classes that changed significantly in relative abundance with time.

**Fig. S6.** Sum of bulk abundances with selected phylum for responder OTUs.

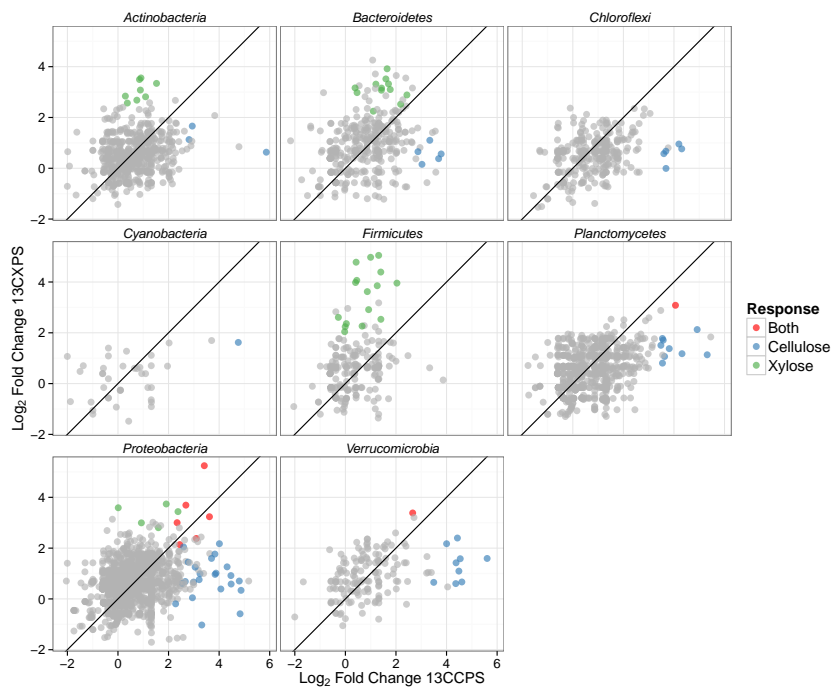


Fig. S7. Maximum \log_2 fold change in response to labeled substrate incorporation for each substrate and all OTUs that pass sparsity filtering in both substrate analyses. Points colored by response. Line has slope of 1 with intercept at the origin. OTUs falling in the top-right quadrant responded to both substrates while those in the top-left and bottom-right responded to ^{13}C -xylose and ^{13}C -cellulose, respectively.

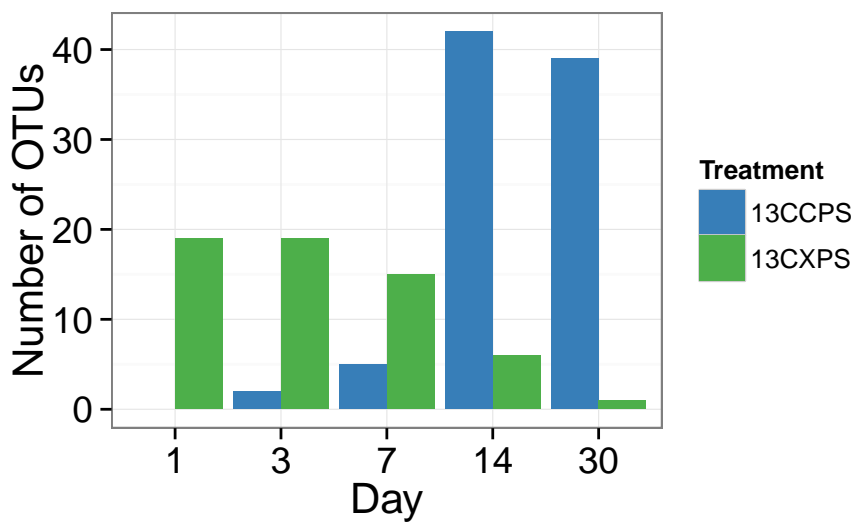


Fig. S8. Counts of responders to each isotopically labeled substrate (cellulose and xylose) over time.

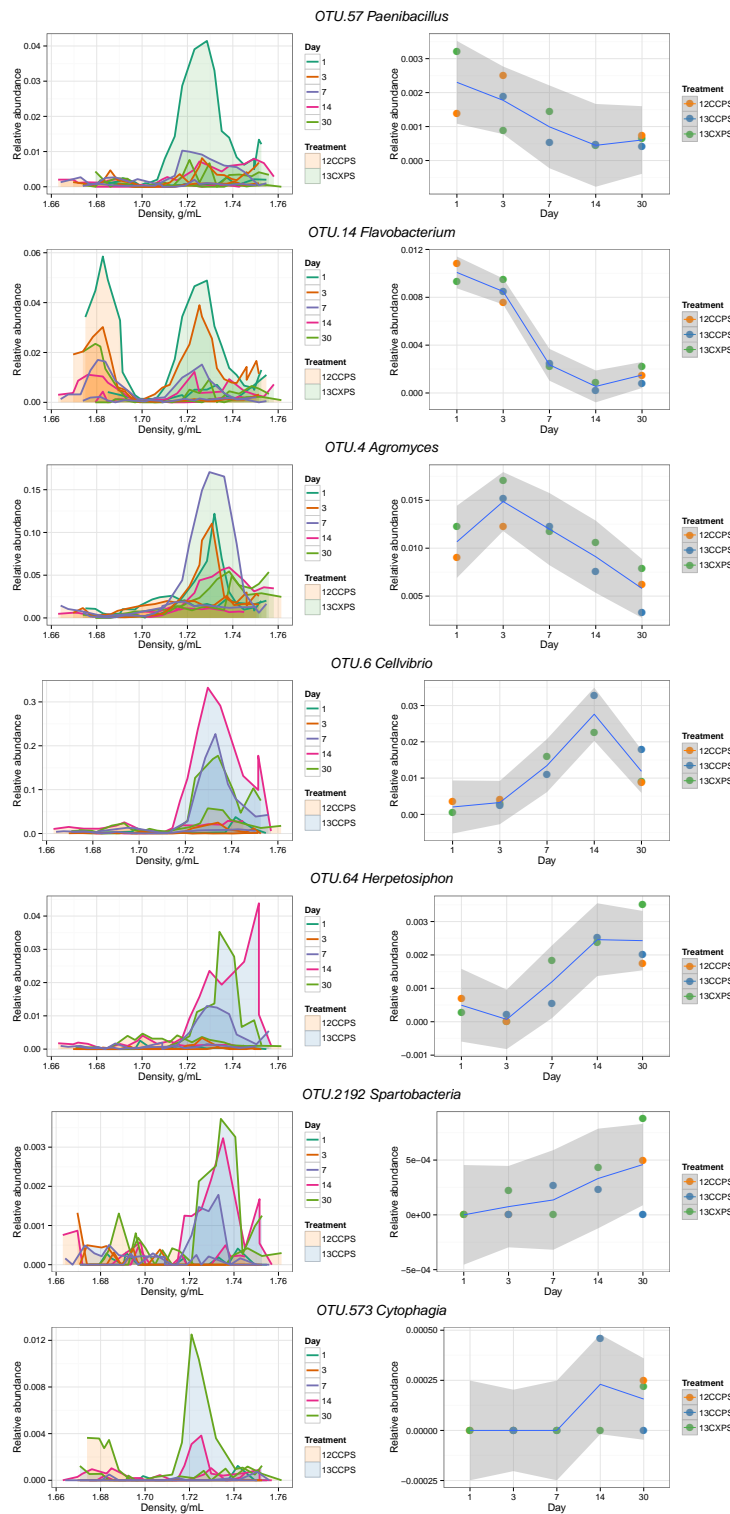


Fig. S9. The left column shows DNA-SIP density fraction relative abundances for all gradients for each of the OTUs. Gradient profiles are shaded by treatment where orange represents “control” profiles, blue “¹³C-cellulose”, and green “¹³C-xylose.” The right column shows the abundance of each OTU in non-fractionated DNA (i.e. the DNA that was subsequently fractionated on the density gradient). Enrichment in the heavy end of the gradient in ¹³C treatments indicates an OTU has ¹³C-labeled DNA that is greater in buoyant density than it would be unlabeled.

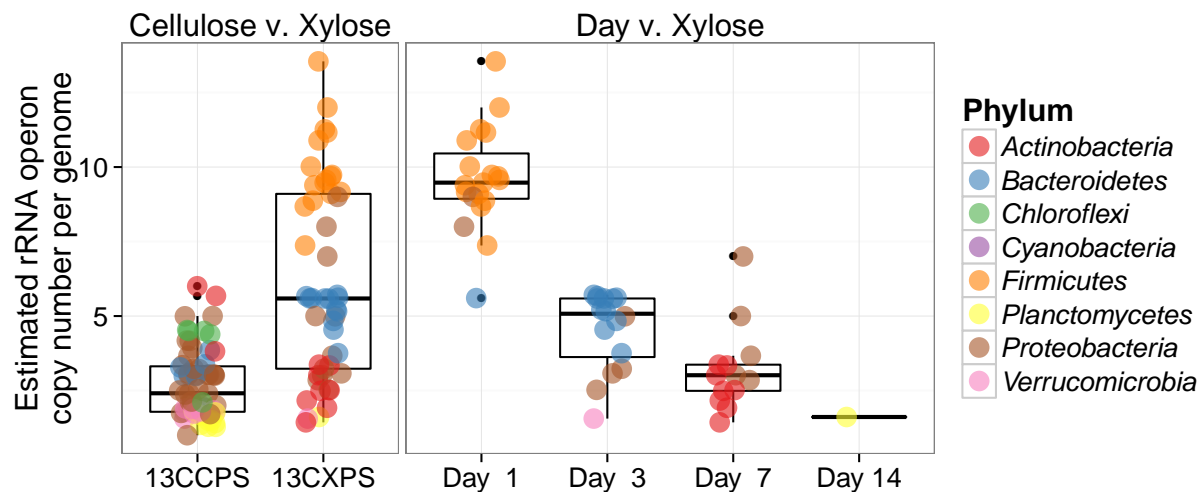


Fig. S10. Estimated rRNA operon copy number per genome for ^{13}C responding OTUs. Panel titles indicate which labeled substrate(s) are depicted.

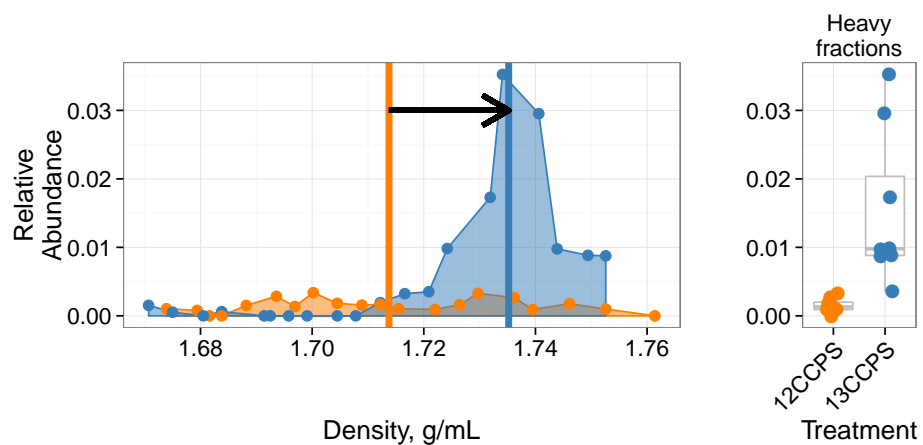


Fig. S11. Density profile for a single ^{13}C -cellulose “responder” OTU in the labeled gradient, blue, and the control gradient, orange. Vertical lines show center of mass for each density profile and arrow denotes the magnitude and direction of the BD shift upon labeling. Panel at right shows relative abundance values in the heavy fractions for each gradient.

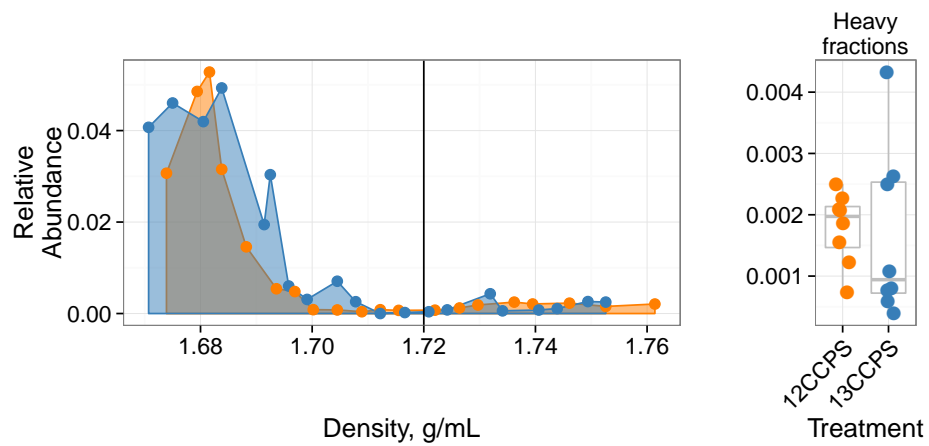


Fig. S12. Density profile for a single ^{13}C -cellulose "non-responder" OTU in the labeled gradient, blue, and the control gradient, orange. Vertical line shows where "heavy" fractions begin as defined in our analysis. Panel at right shows relative abundance values in the heavy fractions for each gradient.

Table S1: ^{13}C -xylose responders BLAST against Living Tree Project

OTU ID	Fold change ^a	Day ^b	All days ^c	Top BLAST hits	BLAST %ID	Phylum;Class;Order
OTU.1040	4.78	1	1	<i>Paenibacillus daejeonensis</i>	100.0	<i>Firmicutes Bacilli Bacillales</i>
OTU.1069	3.85	1	1	<i>Paenibacillus terrigena</i>	100.0	<i>Firmicutes Bacilli Bacillales</i>
OTU.107	2.25	3	3	<i>Flavobacterium sp. 15C3</i> , <i>Flavobacterium banpakuense</i>	99.54	<i>Bacteroidetes Flavobacteria Flavobacterales</i>
OTU.11	5.25	7	7	<i>Stenotrophomonas pavani</i> , <i>Stenotrophomonas maltophilia</i> , <i>Pseudomonas geniculata</i>	99.54	<i>Proteobacteria Gammaproteobacteria Xanthomonadales</i>
OTU.131	3.07	3	3	<i>Flavobacterium fluvii</i> , <i>Flavobacterium bacterium HMD1033</i> , <i>Flavobacterium sp. HMD1001</i>	100.0	<i>Bacteroidetes Flavobacteria Flavobacterales</i>
OTU.14	3.92	3	1, 3	<i>Flavobacterium oncorhynchi</i> , <i>Flavobacterium glycines</i> , <i>Flavobacterium succinicans</i>	99.09	<i>Bacteroidetes Flavobacteria Flavobacterales</i>
OTU.150	3.08	14	14	No hits of at least 90% identity	86.76	<i>Planctomycetes Planctomycetacia Planctomycetales</i>
OTU.159	3.16	3	3	<i>Flavobacterium hibernum</i>	98.17	<i>Bacteroidetes Flavobacteria Flavobacterales</i>
OTU.165	2.38	3	3	<i>Rhizobium skieniewicense</i> , <i>Rhizobium vignae</i> , <i>Rhizobium larrymoorei</i> , <i>Rhizobium alkalisolii</i> , <i>Rhizobium galegae</i> , <i>Rhizobium huautlense</i>	100.0	<i>Proteobacteria Alphaproteobacteria Rhizobiales</i>
OTU.183	3.31	3	3	No hits of at least 90% identity	89.5	<i>Bacteroidetes Sphingobacteriia Sphingobacterales</i>
OTU.19	2.14	7	7	<i>Rhizobium alamii</i> , <i>Rhizobium mesosinicium</i> , <i>Rhizobium mongolense</i> , <i>Arthrobacter viscosus</i> , <i>Rhizobium sullae</i> , <i>Rhizobium yanglingense</i> , <i>Rhizobium loessense</i>	99.54	<i>Proteobacteria Alphaproteobacteria Rhizobiales</i>
OTU.2040	2.91	1	1	<i>Paenibacillus pectinilyticus</i>	100.0	<i>Firmicutes Bacilli Bacillales</i>
OTU.22	2.8	7	7, 14	<i>Paracoccus sp. NB88</i>	99.09	<i>Proteobacteria Alphaproteobacteria Rhodobacterales</i>
OTU.2379	3.1	3	3	<i>Flavobacterium pectinovorum</i> , <i>Flavobacterium sp. CS100</i>	97.72	<i>Bacteroidetes Flavobacteria Flavobacterales</i>
OTU.24	2.81	7	7	<i>Cellulomonas aerilata</i> , <i>Cellulomonas humilata</i> , <i>Cellulomonas terrae</i> , <i>Cellulomonas soli</i> , <i>Cellulomonas xylanilytica</i>	100.0	<i>Actinobacteria Micrococcales Cellulomonadaceae</i>
OTU.241	3.38	3	3, 14	No hits of at least 90% identity	87.73	<i>Verrucomicrobia Spartobacteria Chthoniobacterales</i>
OTU.244	3.08	7	7	<i>Cellulosimicrobium funkei</i> , <i>Cellulosimicrobium terreum</i>	100.0	<i>Actinobacteria Micrococcales Promicromonosporaceae</i>
OTU.252	3.34	7	7	<i>Promicromonospora thailandica</i>	100.0	<i>Actinobacteria Micrococcales Promicromonosporaceae</i>
OTU.267	4.97	1	1	<i>Paenibacillus pabuli</i> , <i>Paenibacillus tundrae</i> , <i>Paenibacillus taichungensis</i> , <i>Paenibacillus xylohexedens</i> , <i>Paenibacillus xylanilyticus</i>	100.0	<i>Firmicutes Bacilli Bacillales</i>
OTU.277	3.52	3	3	<i>Solibius ginsengiterrae</i>	95.43	<i>Bacteroidetes Sphingobacteriia Sphingobacterales</i>

Table S1 – continued from previous page

OTU ID	Fold change	Day	All days	Top BLAST hits	BLAST %ID	Phylum;Class;Order
OTU.290	3.59	1	1	<i>Pantoea spp.</i> , <i>Kluyvera spp.</i> , <i>Klebsiella spp.</i> , <i>Erwinia spp.</i> , <i>Enterobacter spp.</i> , <i>Buttiauxella spp.</i>	100.0	<i>Proteobacteria</i> <i>Gammaproteobacteria</i> <i>Enterobacteriales</i>
OTU.3	2.61	1	1	[<i>Brevibacterium</i>] <i>frigoritolerans</i> , <i>Bacillus sp. LMG 20238</i> , <i>Bacillus coahuilensis m4-4</i> , <i>Bacillus simplex</i>	100.0	<i>Firmicutes</i> <i>Bacilli</i> <i>Bacillales</i>
OTU.319	3.98	1	1	<i>Paenibacillus xinjiangensis</i>	97.25	<i>Firmicutes</i> <i>Bacilli</i> <i>Bacillales</i>
OTU.32	3.0	3	3, 7, 14	<i>Sandaracinus amyloyticus</i>	94.98	<i>Proteobacteria</i> <i>Deltaproteobacteria</i> <i>Myxococcales</i>
OTU.335	2.53	1	1	<i>Paenibacillus thailandensis</i>	98.17	<i>Firmicutes</i> <i>Bacilli</i> <i>Bacillales</i>
OTU.346	3.44	3	3	<i>Pseudoduganella violaceinigra</i>	99.54	<i>Proteobacteria</i> <i>Betaproteobacteria</i> <i>Burkholderiales</i>
OTU.3507	2.36	1	1	<i>Bacillus spp.</i>	98.63	<i>Firmicutes</i> <i>Bacilli</i> <i>Bacillales</i>
OTU.3540	2.52	3	3	<i>Flavobacterium terrigena</i>	99.54	<i>Bacteroidetes</i> <i>Flavobacteria</i> <i>Flavobacteriales</i>
OTU.360	2.98	3	3	<i>Flavisolibacter ginsengisoli</i>	95.0	<i>Bacteroidetes</i> <i>Sphingobacteriia</i> <i>Sphingobacteriales</i>
OTU.369	5.05	1	1	<i>Paenibacillus sp. D75</i> , <i>Paenibacillus glycansilyticus</i>	100.0	<i>Firmicutes</i> <i>Bacilli</i> <i>Bacillales</i>
OTU.37	2.68	7	7	<i>Phycicola gilvus</i> , <i>Microterricola viridarii</i> , <i>Frigoribacterium faeni</i> , <i>Frondihabitans sp. RS-15</i> , <i>Frondihabitans australicus</i>	100.0	<i>Actinobacteria</i> <i>Micrococcales</i> <i>Microbacteriaceae</i>
OTU.394	4.06	1	1	<i>Paenibacillus pocheonensis</i>	100.0	<i>Firmicutes</i> <i>Bacilli</i> <i>Bacillales</i>
OTU.4	2.84	7	7, 14	<i>Agromyces ramosus</i>	100.0	<i>Actinobacteria</i> <i>Micrococcales</i> <i>Microbacteriaceae</i>
OTU.4446	3.49	7	7	<i>Catenuloplanes niger</i> , <i>Catenuloplanes castaneus</i> , <i>Catenuloplanes atrovinosus</i> , <i>Catenuloplanes crispus</i> , <i>Catenuloplanes nepalensis</i> , <i>Catenuloplanes japonicus</i>	97.72	<i>Actinobacteria</i> <i>Frankiales</i> <i>Nakamurellaceae</i>
OTU.4743	2.24	1	1	<i>Lysinibacillus fusiformis</i> , <i>Lysinibacillus sphaericus</i>	99.09	<i>Firmicutes</i> <i>Bacilli</i> <i>Bacillales</i>
OTU.48	2.99	1	1, 3	<i>Aeromonas spp.</i>	100.0	<i>Proteobacteria</i> <i>Gammaproteobacteria</i> <i>aaa34a10</i>
OTU.5	3.69	7	7	<i>Delftia tsuruhatensis</i> , <i>Delftia lacustris</i>	100.0	<i>Proteobacteria</i> <i>Betaproteobacteria</i> <i>Burkholderiales</i>
OTU.5284	3.56	7	7	<i>Isoptericola nanjingensis</i> , <i>Isoptericola hypogaeus</i> , <i>Isoptericola variabilis</i>	98.63	<i>Actinobacteria</i> <i>Micrococcales</i> <i>Promicromonosporaceae</i>
OTU.5603	3.96	1	1	<i>Paenibacillus uliginis</i>	100.0	<i>Firmicutes</i> <i>Bacilli</i> <i>Bacillales</i>
OTU.57	4.39	1	1, 3, 7, 14, 30	<i>Paenibacillus castaneae</i>	98.62	<i>Firmicutes</i> <i>Bacilli</i> <i>Bacillales</i>
OTU.5906	3.16	3	3	<i>Terrimonas sp. M-8</i>	96.8	<i>Bacteroidetes</i> <i>Sphingobacteriia</i> <i>Sphingobacteriales</i>
OTU.6	3.24	3	3	<i>Cellvibrio fulvus</i>	100.0	<i>Proteobacteria</i> <i>Gammaproteobacteria</i> <i>Pseudomonadales</i>

Table S1 – continued from previous page

OTU ID	Fold change	Day	All days	Top BLAST hits	BLAST %ID	Phylum;Class;Order
OTU.62	2.57	7	7	<i>Nakamurella flava</i>	100.0	<i>Actinobacteria Frankiales Nakamurellaceae</i>
OTU.6203	3.32	3	3	<i>Flavobacterium granuli</i> , <i>Flavobacterium glaciei</i>	100.0	<i>Bacteroidetes Flavobacteria Flavobacteriales</i>
OTU.68	3.74	7	7	<i>Shigella flexneri</i> , <i>Escherichia fergusonii</i> , <i>Escherichia coli</i> , <i>Shigella sonnei</i>	100.0	<i>Proteobacteria Gammaproteobacteria Enterobacteriales</i>
OTU.760	2.89	3	3	<i>Dyadobacter hamtensis</i>	98.63	<i>Bacteroidetes Cytophagia Cytophagales</i>
OTU.8	2.26	1	1	<i>Bacillus niaci</i>	100.0	<i>Firmicutes Bacilli Bacillales</i>
OTU.843	3.62	1	1	<i>Paenibacillus agarizedens</i>	100.0	<i>Firmicutes Bacilli Bacillales</i>
OTU.9	2.04	1	1	<i>Bacillus megaterium</i> , <i>Bacillus flexus</i>	100.0	<i>Firmicutes Bacilli Bacillales</i>

^a Maximum observed \log_2 of fold change.^b Day of maximum fold change.^c All response days.

Table S2: ¹³C-cellulose responders BLAST against Living Tree Project

OTU ID	Fold change ^a	Day ^b	All days ^c	Top BLAST hits	BLAST %ID	Phylum;Class;Order
OTU.100	2.66	14	14	<i>Pseudoxanthomonas sacheonensis</i> , <i>Pseudoxanthomonas dokdonensis</i>	100.0	<i>Proteobacteria</i> <i>Gammaproteobacteria</i> <i>Xanthomonadales</i>
OTU.1023	4.61	30	30	No hits of at least 90% identity	80.54	<i>Verrucomicrobia</i> <i>Spartobacteria</i> <i>Chthoniobacterales</i>
OTU.1065	5.31	14	14, 30	No hits of at least 90% identity	84.55	<i>Planctomycetes</i> <i>Planctomycetacia</i> <i>Planctomycetales</i>
OTU.1087	4.32	14	14, 30	<i>Devasia soli</i> , <i>Devasia crocina</i> , <i>Devasia riboflavina</i>	99.09	<i>Proteobacteria</i> <i>Alphaproteobacteria</i> <i>Rhizobiales</i>
OTU.1094	3.69	30	30	<i>Sporocytophaga myxococcoides</i>	99.55	<i>Bacteroidetes</i> <i>Cytophagia</i> <i>Cytophagales</i>
OTU.11	3.41	14	14	<i>Stenotrophomonas pavani</i> i, <i>Stenotrophomonas maltophilia</i> , <i>Pseudomonas geniculata</i>	99.54	<i>Proteobacteria</i> <i>Gammaproteobacteria</i> <i>Xanthomonadales</i>
OTU.114	2.78	14	14	<i>Herbaspirillum sp. SUEMI03</i> , <i>Herbaspirillum sp. SUEMI10</i> , <i>Oxalicibacterium solurbis</i> , <i>Herminiaimonas fonticola</i> , <i>Oxalicibacterium horti</i>	100.0	<i>Proteobacteria</i> <i>Betaproteobacteria</i> <i>Burkholderiales</i>
OTU.119	3.31	14	14, 30	<i>Brevundimonas alba</i>	100.0	<i>Proteobacteria</i> <i>Alphaproteobacteria</i> <i>Caulobacterales</i>
OTU.120	4.76	14	14, 30	<i>Vampirovibrio chlorellavorus</i>	94.52	<i>Cyanobacteria</i> <i>SM1D11</i> uncultured-bacterium
OTU.1204	4.32	30	30	<i>Planctomyces limnophilus</i>	91.78	<i>Planctomycetes</i> <i>Planctomycetacia</i> <i>Planctomycetales</i>
OTU.1312	4.07	30	30	<i>Paucimonas lemoignei</i>	99.54	<i>Proteobacteria</i> <i>Betaproteobacteria</i> <i>Burkholderiales</i>
OTU.132	2.81	14	14	<i>Streptomyces spp.</i>	100.0	<i>Actinobacteria</i> <i>Streptomycetales</i> <i>Streptomycetaceae</i>
OTU.150	4.06	14	14	No hits of at least 90% identity	86.76	<i>Planctomycetes</i> <i>Planctomycetacia</i> <i>Planctomycetales</i>
OTU.1533	3.43	30	30	No hits of at least 90% identity	82.27	<i>Verrucomicrobia</i> <i>Spartobacteria</i> <i>Chthoniobacterales</i>
OTU.154	3.24	14	14	<i>Pseudoxanthomonas mexicana</i> , <i>Pseudoxanthomonas japonensis</i>	100.0	<i>Proteobacteria</i> <i>Gammaproteobacteria</i> <i>Xanthomonadales</i>
OTU.165	3.1	14	14	<i>Rhizobium skieniewicense</i> , <i>Rhizobium vignae</i> , <i>Rhizobium larrymoorei</i> , <i>Rhizobium alkalisolii</i> , <i>Rhizobium galegae</i> , <i>Rhizobium huautlense</i>	100.0	<i>Proteobacteria</i> <i>Alphaproteobacteria</i> <i>Rhizobiales</i>
OTU.1754	4.48	14	14	<i>Asticcacaulis biprosthecum</i> , <i>Asticcacaulis benevestitus</i>	96.8	<i>Proteobacteria</i> <i>Alphaproteobacteria</i> <i>Caulobacterales</i>
OTU.185	4.37	14	14, 30	No hits of at least 90% identity	85.14	<i>Verrucomicrobia</i> <i>Spartobacteria</i> <i>Chthoniobacterales</i>
OTU.19	2.44	14	14	<i>Rhizobium alamii</i> , <i>Rhizobium mesosinicum</i> , <i>Rhizobium mongolense</i> , <i>Arthrobacter viscosus</i> , <i>Rhizobium sullae</i> , <i>Rhizobium yanglingense</i> , <i>Rhizobium loessense</i>	99.54	<i>Proteobacteria</i> <i>Alphaproteobacteria</i> <i>Rhizobiales</i>

Table S2 – continued from previous page

OTU ID	Fold change	Day	All days	Top BLAST hits	BLAST %ID	Phylum;Class;Order
OTU.2192	3.49	30	14, 30	No hits of at least 90% identity	83.56	Verrucomicrobia Spartobacteria Chthoniobacterales
OTU.228	2.54	30	30	<i>Sorangium cellulosum</i>	98.17	Proteobacteria Deltaproteobacteria Myxococcales
OTU.241	2.66	14	14	No hits of at least 90% identity	87.73	Verrucomicrobia Spartobacteria Chthoniobacterales
OTU.257	2.94	14	14	<i>Lentzea waywayandensis</i> , <i>Lentzea flaviverrucosa</i>	100.0	Actinobacteria Pseudonocardiales Pseudonocardiaceae
OTU.266	4.54	30	14, 30	No hits of at least 90% identity	83.64	Verrucomicrobia Spartobacteria Chthoniobacterales
OTU.28	2.59	14	14	<i>Rhizobium giardinii</i> , <i>Rhizobium tubonense</i> , <i>Rhizobium tibeticum</i> , <i>Rhizobium mesoamericanum CCGE 501</i> , <i>Rhizobium herbae</i> , <i>Rhizobium endophyticum</i>	99.54	Proteobacteria Alphaproteobacteria Rhizobiales
OTU.285	3.55	30	14, 30	<i>Blastopirellula marina</i>	90.87	Planctomycetes Planctomycetacia Planctomycetales
OTU.32	2.34	3	3	<i>Sandaracinus amyloyticus</i>	94.98	Proteobacteria Deltaproteobacteria Myxococcales
OTU.327	2.99	14	14	<i>Asticcacaulis biprostheciun</i> , <i>Asticcacaulis benevestitus</i>	98.63	Proteobacteria Alphaproteobacteria Caulobacterales
OTU.351	3.54	14	14, 30	<i>Pirellula staleyi DSM 6068</i>	91.86	Planctomycetes Planctomycetacia Planctomycetales
OTU.3594	3.83	30	30	<i>Chondromyces robustus</i>	90.41	Proteobacteria Deltaproteobacteria Myxococcales
OTU.3775	3.88	14	14	<i>Devasia glacialis</i> , <i>Devasia chinhatensis</i> , <i>Devasia geoensis</i> , <i>Devasia yakushimensis</i>	98.63	Proteobacteria Alphaproteobacteria Rhizobiales
OTU.429	3.7	30	14, 30	<i>Devasia limi</i> , <i>Devasia psychrophila</i>	97.72	Proteobacteria Alphaproteobacteria Rhizobiales
OTU.4322	4.19	14	7, 14, 30	No hits of at least 90% identity	89.14	Chloroflexi Herpetosiphonales Herpetosiphonaceae
OTU.442	3.05	30	30	<i>Chondromyces robustus</i>	92.24	Proteobacteria Deltaproteobacteria Myxococcales
OTU.465	3.79	30	30	<i>Ohtaekwangia kribbensis</i>	92.73	Bacteroidetes Cytophagia Cytophagales
OTU.473	3.58	14	14	<i>Pirellula staleyi DSM 6068</i>	90.91	Planctomycetes Planctomycetacia Planctomycetales
OTU.484	4.92	14	14, 30	No hits of at least 90% identity	89.09	Planctomycetes Planctomycetacia Planctomycetales
OTU.5	2.69	14	14	<i>Delftia tsuruhatensis</i> , <i>Delftia lacustris</i>	100.0	Proteobacteria Betaproteobacteria Burkholderiales
OTU.518	4.8	14	14	<i>Hydrogenophaga intermedia</i>	100.0	Proteobacteria Betaproteobacteria Burkholderiales
OTU.5190	3.6	30	14, 30	No hits of at least 90% identity	88.13	Chloroflexi Herpetosiphonales Herpetosiphonaceae
OTU.541	4.49	30	30	No hits of at least 90% identity	84.23	Verrucomicrobia Spartobacteria Chthoniobacterales
OTU.5539	4.01	14	14	<i>Devasia subaequoris</i>	98.17	Proteobacteria Alphaproteobacteria Rhizobiales
OTU.573	3.03	30	30	<i>Adhaeribacter aerophilus</i>	92.76	Bacteroidetes Cytophagia Cytophagales

Table S2 – continued from previous page

OTU ID	Fold change	Day	All days	Top BLAST hits	BLAST %ID	Phylum;Class;Order
OTU.6	3.62	7	3, 7, 14	<i>Cellvibrio fulvus</i>	100.0	Proteobacteria Gammaproteobacteria Pseudomonadales
OTU.600	3.48	30	30	No hits of at least 90% identity	80.37	Planctomycetes Planctomycetacia Planctomycetales
OTU.6062	4.83	30	30	<i>Dokdonella sp. DC-3</i> , <i>Luteibacter rhizovicinus</i>	97.26	Proteobacteria Gammaproteobacteria Xanthomonadales
OTU.627	4.43	14	14	<i>Verrucomicrobiaceae bacterium DC2a-G7</i>	100.0	Verrucomicrobia Verrucomicrobiae Verrucomicrobiales
OTU.633	3.84	30	30	No hits of at least 90% identity	89.5	Proteobacteria Deltaproteobacteria Myxococcales
OTU.638	4.0	30	30	<i>Luteolibacter sp. CCTCC AB 2010415</i> , <i>Luteolibacter algae</i>	93.61	Verrucomicrobia Verrucomicrobiae Verrucomicrobiales
OTU.64	4.31	14	7, 14, 30	No hits of at least 90% identity	89.5	Chloroflexi Herpetosiphonales Herpetosiphonaceae
OTU.663	3.63	30	30	<i>Pirellula staleyi DSM 6068</i>	90.87	Planctomycetes Planctomycetacia Planctomycetales
OTU.669	3.34	30	30	<i>Ohtaekwangia koreensis</i>	92.69	Bacteroidetes Cytophagia Cytophagales
OTU.670	2.87	30	30	<i>Adhaeribacter aerophilus</i>	91.78	Bacteroidetes Cytophagia Cytophagales
OTU.766	3.21	14	14, 30	<i>Devosia insulae</i>	99.54	Proteobacteria Alphaproteobacteria Rhizobiales
OTU.83	5.61	14	7, 14, 30	<i>Luteolibacter sp. CCTCC AB 2010415</i>	97.72	Verrucomicrobia Verrucomicrobiae Verrucomicrobiales
OTU.862	5.87	14	14	<i>Allotkutznheria albata</i>	100.0	Actinobacteria Pseudonocardiales Pseudonocardiaceae
OTU.899	2.28	30	30	<i>Enhygromyxa salina</i>	97.72	Proteobacteria Deltaproteobacteria Myxococcales
OTU.90	2.94	14	14, 30	<i>Sphingopyxis panaciterra</i> , <i>Sphingopyxis chilensis</i> , <i>Sphingopyxis sp. BZ30</i> , <i>Sphingomonas sp.</i>	100.0	Proteobacteria Alphaproteobacteria Sphingomonadales
OTU.900	4.87	14	14	<i>Brevundimonas vesicularis</i> , <i>Brevundimonas nasdae</i>	100.0	Proteobacteria Alphaproteobacteria Caulobacterales
OTU.971	3.68	30	30	No hits of at least 90% identity	78.57	Chloroflexi Anaerolineae Anaerolineales
OTU.98	3.68	14	7, 14, 30	No hits of at least 90% identity	88.18	Chloroflexi Herpetosiphonales Herpetosiphonaceae
OTU.982	4.47	14	14	<i>Devosia neptuniae</i>	100.0	Proteobacteria Alphaproteobacteria Rhizobiales

^a Maximum observed \log_2 of fold change.^b Day of maximum fold change.^c All response days.

Supplemental Information

Contents

1 Supplemental Methods	1
1.1 Soil Collection and Preparation	1
1.2 Cellulose production	2
1.3 Soil microcosms	2
1.4 Nucleic acid extraction	3
1.5 Isopycnic centrifugation and fractionation	3
1.6 DNA Sequencing	4
1.6.1 PCR amplification of SSU rRNA genes	4
1.6.2 DNA sequence quality control	4
1.6.3 OTU binning	4
1.6.4 Phylogenetic reconstruction	5
1.7 OTU characteristics	5
1.7.1 Identifying ^{13}C responders	5
1.7.2 Estimating rrn copy number	5
1.7.3 NRI, NTI, and consenTRAIT	5
1.7.4 Buoyant density shift estimates	5
1.7.5 Finding cultured relatives of OTUs	6
1.7.6 OTU changes in relative abundance with time	6
1.8 Sequencing and density fractionation statistics	6

1 Supplemental Methods

1.1 Soil Collection and Preparation

We collected soils from an organic farm in Penn Yan, New York. Soils were Honoeye/Lima, a silty clay loam on calcareous bedrock. To get a field average, cores (5 cm diameter x 10 cm depth) were collected in duplicate from six different sampling locations around the field using a slide hammer bulk density sampler (coordinates: (1) N 42° 40.288 W 77° 02.438, (2) N 42° 40.296 W 77° 02.438, (3) N 42° 40.309 W 77° 02.445, (4) N 42° 40.333 W 77° 02.425, (5) N 42° 40.340 W 77° 02.420, (6) N 42° 40.353 W 77° 02.417) on November 21, 2011. Soil cores were sieved (2mm), homogenized by mixing, and stored at 4C until preincubation (within 1-2 week of collection). Carbon and nitrogen content were previously measured for these soils [1]. Reported soil C values for the organic field were 12.15 (\pm s.d. 0.78) mg C g $^{-1}$ dry soil and 1.16 (\pm s.d. 0.13) mg N g $^{-1}$ dry soil.

1.2 Cellulose production

Bacterial cellulose was produced by *Gluconoacetobacter xylinus* grown in Heo and Son [2] minimal media (HS medium) made with 0.1% glucose and without inositol. For the production of ^{13}C -cellulose, $^{13}\text{C}_6\text{-D-glucose}$, 99 atom % ^{13}C (Isotec) was used. Cellulose was produced in 1L Erlenmeyer flasks containing 100 mL HS medium inoculated with three colonies of *Gluconoacetobacter xylinus* grown on HS agar plates. Flasks were incubated statically in the dark at 30°C for 2-3 weeks. Cellulose pellicles were decanted, rinsed with deionized water, suspended in two volumes of 1% alconox, and then autoclaved. Cellulose pellicles were purified by dialysis for 12 hr in 1 L deionized water and dialysis was repeated 10 times. Harvested pellicles were dried overnight (60°C), cut into pieces, and ground to 53 μm - 250 μm using 5100 Mixer/Mill (SPEX SamplePrep, Metuchen, NJ) and dry sieve. The particulate size range was selected to be representative of particulate organic matter in soils (3).

The purity of ground cellulose was checked by biological assay, Benedict's reducing sugars assay, Bradford assay, and isotopic analysis. *E.coli* is not able to use cellulose as a C source but is capable of growth on a variety of nutrients available in the Heo and Son medium. The biological assay consisted of *E. coli* inoculated into minimal M9 media which lacked a C source and was supplemented with either: (1) 0.01% glucose, (2) 2.5 mg purified, ground cellulose, (3) 25 mg purified, ground cellulose, (4) 25 mg purified, ground cellulose and 0.01% glucose. Growth in media was checked by spectrometer (OD_{450}). No measurable growth was observed with either 2 mg or 25 mg cellulose, indicating absence of contaminating nutrients that can support growth of *E. coli*. In addition, the presence of 25 mg cellulose did not inhibit the growth of *E.coli* cultures provided with glucose (relative to control), indicating the absence of compounds in the purified cellulose that could inhibit microbial growth.

Purified cellulose was also assayed for residual proteins and sugars using Bradford and Benedict's assays, respectively. Bradford assay was performed as in [3] with a standard curve ranging from 0 - 2000 $\mu\text{g ml}^{-1}$ BSA. Ground, purified cellulose contained 6.92 $\mu\text{g protein mg cellulose}^{-1}$ (*i.e.* 99.31% purity). Reducing sugars were not detected in cellulose using Benedict's reducing sugar assay [4] tested at 10 mg cellulose ml^{-1} . Finally, ^{13}C -cellulose had an average $96\% \pm 5$ (s.d.) degree of ^{13}C labeling as determined by isotopic analysis (UCDavis Stable Isotope Facility).

1.3 Soil microcosms

Microcosms were created by adding 10 g d.w. sieved soil to a 250 mL Erlenmeyer flask capped with a butyl rubber stopper. The headspace was flushed with air every 3 days which was sufficient to prevent anoxia (data not shown). Microcosms were pre-incubated at room temperature for 2 weeks until the soil respiration rate (determined by GCMS measurement of head space CO_2) had stabilized. Sieving causes a transient increase in soil respiration rate presumably due to the liberation of fresh labile soil organic matter [5]. Pre-incubation ensures that this labile organic matter is consumed and/or stabilized prior to the beginning of the experiment. Respiration rate (CO_2) stabilized after 10 days (data not shown).

Three parallel treatments were established. Each treatment received the same amendment, where the only difference was the isotopically labeled component in the amendment. Specifically, we made unlabeled control treatment and treatments that substituted either ^{13}C -cellulose (synthesized as described above) or $^{13}\text{C}_5\text{-D-xylose}$, 98 atom % ^{13}C (Isotec) for their unlabeled equivalents. The molecular composition of the amendment was designed to approximate switchgrass biomass with hemicellulose replaced by its constituent monomers [6, 7]. The amendment was added at 5.3

mg g^{-1} d.w. soil which is representative of natural concentrations in soil during early phases of decomposition [8]. The amendment contained by mass: 38% cellulose, 23% lignin, 20% xylose, 3% arabinose, 1% galactose, 1% glucose, and 0.5% mannose, with the remaining 13.5% composed of amino acids (Teknova C0705) and a basal salt mixture (Murashige and Skoog, Sigma Aldrich M5524). The amendment had a C:N ratio of 10. Cellulose (2 mg cellulose g^{-1} d.w. soil) and lignin (1.2 mg lignin g^{-1} d.w. soil) were uniformly distributed over the soil surface as a powder and the remaining constituents were added in solution in a volume of 0.12 ml g^{-1} d.w. soil. The volume of liquid was determined in relation to soil moisture to achieve 50% water holding capacity. Water holding capacity of 50% was chosen, in relation to the texture for this soil, to achieve approximately 70% water filled pore space, which is the optimal water content for respiration [9]. A total of 12 microcosms were established per treatment. Microcosms were sampled destructively on days 1, 3, 7, 14, and 30 and soils were frozen at -80 °C. The cellulose treatment was not sampled on day 1 because it was not expected that significant cellulose metabolism would have occurred within this time. The abbreviation 13CXPS refers to the 13C-xylose treatment (13C Xylose Plant Simulant), 13CCPS refers to the 13C-cellulose treatment and 12CCPS refers to the unlabeled control. A subset of soil from each sample was reserved for isotopic analysis at the Cornell University Stable Isotope Laboratory to determine the mass of ^{13}C remaining in soil.

1.4 Nucleic acid extraction

Nucleic acids were extracted from 0.25 g soil using a modified Griffiths protocol [10]. Cells were lysed by bead beating for 1 min at 5.5 ms^{-1} in 2mL lysis tubes containing 0.5 g of 0.1 mm diameter silica/zirconia beads (treated at 300C for 4 hours to remove RNases), 0.5 mL extraction buffer (240 mM Phosphate buffer 0.5% N-lauryl sarcosine), and 0.5 mL phenol-chloroform-isoamyl alcohol (25:24:1) for 1 min at 5.5 ms^{-1} . After lysis, 85 uL 5 M NaCl and 60 uL 10% hexadecyltrimethylammonium bromide (CTAB)/0.7 M NaCl were added to lysis tube, vortexed, chilled for 1 min on ice, and centrifuged at 16,000 x g for 5 min at 4C. The aqueous layer was transferred to a new tube and reserved on ice. To increase DNA recovery, the pellet was back extracted with 85 uL 5 M NaCl and 0.5 mL extraction buffer. The aqueous extract was washed with 0.5 mL chloroform:isoamyl alcohol (24:1). Nucleic acids were precipitated by addition of 2 volumes polyethylene glycol solution (30% PEG 8000, 1.6 M NaCl) on ice for 2 hrs, followed by centrifugation at 16,000 x g, 4C for 30 min. The supernatant was discarded and pellets were washed with 1 mL ice cold 70% EtOH. Pellets were air dried, resuspended in 50 uL TE and stored at -20C. To prepare nucleic acid extracts for isopycnic centrifugation as previously described [11], DNA was size selected ($> 4\text{kb}$) using 1% low melt agarose gel and β -agarase I enzyme extraction per manufacturers protocol (New England Biolab, M0392S). Final resuspension of DNA pellet was in 50 μL TE.

1.5 Isopycnic centrifugation and fractionation

We fractionated DNA on density gradients for ^{13}C -xylose treatments (days 1, 3, 7, 14, 30), ^{13}C -cellulose treatments (days 3, 7, 14, 30), and control treatments (days 1, 3, 7, 14, 30). A total of 5 μg DNA was added to each 4.7 mL CsCl density gradient. Density gradient were composed of 1.69 g mL^{-1} CsCl ml^{-1} in gradient buffer solution (pH 8.0 15 mM Tris-HCl, 15 mM EDTA, 15 mM KCl). Centrifugation was performed at 55,000 rpm 20 °C for 66 hr using a TLA-110 rotor in a Bechman Coulter Optima MAX-E ultracentrifuge. Fractions of $\sim 100 \mu\text{L}$ were collected from below by displacing the DNA-CsCl-gradient buffer solution in the centrifugation tube with water

using a syringe pump at a flow rate of $3.3 \mu\text{L s}^{-1}$ [12] into Acroprep 96 filter plate (part no. 5035, Pall Life Sciences). The refractive index of each fraction was measured using a Reichart AR200 digital refractometer modified as previously described to measure a volume of $5 \mu\text{L}$ [11]. Buoyant density was calculated from the refractive index as previously described [11] using the equation $\rho = a\eta - b$, where ρ is the density of the CsCl (g ml^{-1}), η is the measured refractive index, and a and b are coefficient values of 10.9276 and 13.593, respectively, for CsCl at 20C [13] and correcting for non-CsCl salts in the gradient buffer. A total of 35 fractions were collected from each gradient and the average density between fractions was 0.0040 g mL^{-1} . The DNA was desalting by washing with TE (5X 200 μL) in the Acroprep filter wells. DNA was resuspended in 50 μL TE.

1.6 DNA Sequencing

1.6.1 PCR amplification of SSU rRNA genes

SSU rRNA genes were amplified from gradient fractions ($n = 20$ per gradient) and from non-fractionated DNA from soil. Barcoded primers consisted of: 454-specific adapter B, a 10 bp barcode (Reference 90), a 2 bp linker (5-CA-3), and 806R primer for reverse primer (BA806R); and 454-specific adapter A, a 2 bp linker (5-TC-3), and 515F primer for forward primer (BA515F). Each PCR contained 1.25 U l-1 AmpliTaq Gold (Life Technologies, Grand Island, NY; N8080243), 1X Buffer II (100 mM Tris-HCl, 500 mM KCl, pH 8.3), 2.5 mM MgCl₂, 200 M of each dNTP, 0.5 mg ml-1 BSA, 0.2 M BA515F, 0.2 M BA806R, and 10 L of 1:30 DNA template in 25 l total volume). The PCR conditions were 95C for 5min followed by 22 cycles of 95C for 10s, 53C for 30s, and 72C for 30s, followed by a final elongation at 72C for 5 min. Amplification products were checked by 1% agarose gel. Reactions were performed in triplicate and pooled. Amplified DNA was gel purified (1% low melt agarose) using the Wizard SV gel and PCR clean-up system (Promega, Madison, WI; A9281) per manufacturers protocol. Samples were normalized by SequalPrepTM normalization plates (Invitrogen, Carlsbad, CA; A10510) and pooled in equimolar concentration. Amplicons were sequenced on Roche 454 FLX system using titanium chemistry at Selah Genomics (Columbia, SC).

1.6.2 DNA sequence quality control

SSU rRNA gene sequences were initially screened by maximum expected errors at a specific read length threshold [14]. Reads that had more than 0.5 expected errors at a length of 250 nt were discarded. The remaining reads were aligned to the Silva Reference Alignment as provided in the Mothur software package using the Mothur NAST aligner [15, 16]. Reads that did not align to the expected region of the SSU rRNA gene were discarded. After expected error and alignment based quality control. The remaining quality controlled reads were annotated using the UClust taxonomic annotation framework in [17, 18]. We used 97% cluster seeds from the Silva SSU rRNA database (release 111Ref) [19] as reference for taxonomic annotation (provided on the QIIME website) [19]. Quality control screening filtered out 344,472 or 1,720,480 raw sequencing reads. Reads annotated as "Chloroplast", "Eukaryota", "Archaea", "Unassigned" or "mitochondria" were culled from the dataset.

1.6.3 OTU binning

Sequences were distributed into OTUs with a centroid based clustering algorithm (i.e. UPARSE [14]). The centroid selection also included robust chimera screening [14]. OTU centroids were

established at a threshold of 97% sequence identity and non-centroid sequences were mapped back to centroids. Reads that could not be mapped to an OTU centroid at greater than or equal to 97% sequence identity were discarded.

1.6.4 Phylogenetic reconstruction

We used SSU-Align [20, 21] to align SSU rRNA gene sequences. Columns in the alignment that were aligned with poor confidence (< 95% of characters had posterior probability > 95%) were not considered when building the phylogenetic tree. Additionally, the alignment was trimmed to coordinates such that all sequences in the alignment began and ended at the same positions. FastTree [22] was used with default parameters to build the phylogeny. NMDS ordination was performed on weighted Unifrac [23] distances between samples. The Phyloseq [24] wrapper for Vegan [25] (both R packages) was used to compute sample values along NMDS axes. The 'adonis' function in Vegan was used to perform Adonis tests (default parameters) [26].

1.7 OTU characteristics

1.7.1 Identifying ^{13}C responders

Figures S11 and S12 demonstrate raw data for responder and non-responder OTUs, respectively. Responders increased in relative abundance in the heavy fractions due to ^{13}C -labeling of their DNA. As our data is compositional, often OTUs had consistent *relative* abundance across the density gradients. If OTU DNA is positioned in heavy or light fractions, however, due to G+C content and/or ^{13}C -labeling, it spikes in relative abundance near where it is centered. Thus, we identified responders by finding OTUs enriched in heavy fractions of ^{13}C treatment gradients relative to control. This technique accounts for the variation in OTU base abundance and the variation in OTU G+C content (and therefore natural buoyant density) because ^{13}C treatment abundances are always compared to appropriate control abundances.

1.7.2 Estimating *rrn* copy number

We estimated the *rrn* copy number for each OTU as described in (author?) [27] (i.e. we used the code and reference information provided in (author?) [27] directly). In brief, OTU centroid sequences were inserted into a reference SSU rRNA gene phylogeny [28] from organisms of known *rrn* copy number. The *rrn* copy number was then inferred from the phylogenetic placement in the reference phylogeny.

1.7.3 NRI, NTI, and consenTRAIT

NRI and NTI were calculated using the "picante" R package [29]. We used the "independentswap" null model for phylogenetic distribution. The consenTRAIT clade depth for xylose and cellulose responders was calculated using R code used to calculate the metric in (author?) [30] which employs the R "adephylo" package [31].

1.7.4 Buoyant density shift estimates

Upon labeling, DNA from an organism that incorporates exclusively ^{13}C will increase in BD more than DNA from an organism that does not exclusively utilize isotopically labeled C. Therefore, the

magnitude DNA $\Delta\hat{BD}$ indicates substrate specificity given our experimental design as only one substrate was labeled in each amendment (assuming all members of an OTU behave similarly with respect to ^{13}C incorporation). We measured $\Delta\hat{BD}$ as the change in an OTU's density profile center of mass between corresponding control and labeled gradients (Figure S11). Because all gradients did not span the same density range and gradient fractions cannot be taken at specific density positions, we limited our $\Delta\hat{BD}$ analysis to the density range for which fractions were taken for all gradients. Within this density range we linearly interpolated 20 evenly spaced relative abundance values. The center of mass for an OTU along the density gradient was then the density weighted average where weights were the linearly interpolated relative abundance values. $\Delta\hat{BD}$ should not be evaluated on an individual OTU basis as a small number of $\Delta\hat{BD}$ values are observed for each OTU and the variance of the density shift metric at the level of individual OTUs is unknown. It is therefore more informative to compare $\Delta\hat{BD}$ among substrate responder groups. Further, $\Delta\hat{BD}$ values are based on relative abundance profiles and would be distorted in comparison to $\Delta\hat{BD}$ based on absolute DNA concentration profiles and should be interpreted with this transformation in mind. It should also be noted that there was overlap in observed $\Delta\hat{BD}$ between ^{13}C -cellulose and ^{13}C -xylose responder groups.

1.7.5 Finding cultured relatives of OTUs

OTU centroids were compared (BLAST [32, 33]) to sequences in “The All-Species Living Tree” project (LTP). The LTP is a collection of SSU rRNA gene sequences for classified species of Archaea and Bacteria [34]. We used LTP version 115 for analyses in this paper.

1.7.6 OTU changes in relative abundance with time

We identified OTUs that changed in relative abundance over time using DESeq2 [35]. Specifically, we used day treated as an ordered factor as the regressor with LFC of the relative abundance in non-fractionated DNA as the outcome in the general linear model. We used the default DESeq2 base mean independent filtering and disabled the Cook’s cutoff outlier detection. The null model was that abundance did not change with time and we assessed significance at a false discovery rate of 10%.

1.8 Sequencing and density fractionation statistics

Microcosm DNA was density fractionated on CsCl density gradients. We sequenced SSU rRNA gene amplicons from a total of 277 CsCl gradient fractions from 14 CsCl gradients and 12 bulk microcosm DNA samples. The SSU rRNA gene data set contained 1,102,685 total sequences. The average number of sequences per sample was 3,816 (sd 3,629) and 265 samples had over 1,000 sequences. We sequenced SSU rRNA gene amplicons from an average of 19.8 fractions per CsCl gradient (sd 0.57). The average density between fractions was 0.0040 g mL⁻¹. The sequencing effort recovered a total of 5,940 OTUs. 2,943 of the total 5,940 OTUs were observed in bulk samples. We observed 33 unique phylum and 340 unique genus annotations.

References

- [1] Berthrong S-T, Buckley D-H, Drinkwater L-E (2013) Agricultural Management and Labile Carbon Additions Affect Soil Microbial Community Structure and Interact with Carbon and Nitrogen Cycling. *Microb Ecol* 66(1): 158–170.
- [2] Heo M-S, Son H-J (2002) Development of an optimized, simple chemically defined medium for bacterial cellulose production by Acetobacter sp. A9 in shaking cultures. *Biotechnol Appl Biochem* 36(1): 41.
- [3] Bradford M-M (1976) A rapid and sensitive method for the quantitation of microgram quantities of protein utilizing the principle of protein-dye binding. *Analytical Biochemistry* 72(1-2): 248–254.
- [4] Benedict S-R (1909) A reagent for the detection of reducing sugars. *Journal of Biological Chemistry* 5(5): 485–487.
- [5] Datta R, Vranová V, Pavelka M, Rejšek K, Formánek P (2014) Effect of soil sieving on respiration induced by low-molecular-weight substrates. *International Agrophysics* 28(1): ???.
- [6] Yan J, Hu Z, Pu Y, Brummer E-C, Ragauskas A-J (2010) Chemical compositions of four switchgrass populations. *Biomass and Bioenergy* 34(1): 48–53.
- [7] David K, Ragauskas A-J (2010) Switchgrass as an energy crop for biofuel production: A review of its ligno-cellulosic chemical properties. *Energy Environ Sci* 3(9): 1182.
- [8] Schneckenberger K, Demin D, Stahr K, Kuzyakov Y (2008) Microbial utilization and mineralization of ¹⁴C glucose added in six orders of concentration to soil. *Soil Biol Biochem* 40(8): 1981–1988.
- [9] Linn D-M, Doran J-W (1984) Aerobic and Anaerobic Microbial Populations in No-till and Plowed Soils1. *Soil Sci Soc Am J* 48(4): 794.
- [10] Griffiths R-I, Whiteley A-S, O'Donnell A-G, Bailey M-J (2000) Rapid method for coextraction of DNA and RNA from natural environments for analysis of ribosomal DNA- and rRNA-based microbial community composition. *Appl Environ Microbiol* 66(12): 5488–5491.
- [11] Buckley D-H, Huangyutitham V, Hsu S-F, Nelson T-A (2007) Stable isotope probing with ¹⁵N achieved by disentangling the effects of genome G+C content and isotope enrichment on DNA density. *Appl Environ Microbiol* 73(10): 3189–3195.
- [12] Manefield M, Whiteley A-S, Griffiths R-I, Bailey M-J (2002) RNA Stable isotope probing a novel means of linking microbial community function to phylogeny. *Appl Environ Microbiol* 68(11): 5367–5373.
- [13] Birnie G-D (1978) Centrifugal separations in Molecular and cell biology. (Butterworth & Co Publishers Ltd, Boston)
- [14] Edgar R-C (2013) UPARSE: highly accurate OTU sequences from microbial amplicon reads. *Nat. Methods* 10(10): 996–998.

- [15] DeSantis T-Z, Hugenholtz P, Keller K, Brodie E-L, Larsen N, Piceno Y-M, *et al.* (2006) NAST: a multiple sequence alignment server for comparative analysis of 16S rRNA genes. *Nucleic Acids Res* 34(suppl 2): W394–W399.
- [16] Schloss P-D, Westcott S-L, Ryabin T, Hall J-R, Hartmann M, Hollister E-B, *et al.* (2009) Introducing mothur: open-source, platform-independent, community-supported software for describing and comparing microbial communities. *Appl Environ Microbiol* 75(23): 7537–7541.
- [17] Caporaso J-G, Kuczynski J, Stombaugh J, Bittinger K, Bushman F-D, Costello E-K, *et al.* (2010) QIIME allows analysis of high-throughput community sequencing data. *Nat. Methods* 7(5): 335–336.
- [18] Edgar R-C (2010) Search and clustering orders of magnitude faster than BLAST. *Bioinformatics* 26(19): 2460–2461.
- [19] Quast C, Pruesse E, Yilmaz P, Gerken J, Schweer T, Yarza P, *et al.* (2013) The SILVA ribosomal RNA gene database project: improved data processing and web-based tools. *Nucleic Acids Res* 41: D590–596.
- [20] Nawrocki E-P, Kolbe D-L, Eddy S-R (2009) Infernal 1.0: inference of RNA alignments. *Bioinformatics* 25(10): 1335–1337.
- [21] Nawrocki E-P, Eddy S-R (2013) Infernal 1.1: 100-fold faster RNA homology searches. *Bioinformatics* 29(22): 2933–2935.
- [22] Price M-N, Dehal P-S, Arkin A-P (2010) FastTree2 - approximately maximum-likelihood trees for large alignments. *PLoS ONE* 5(3): e9490.
- [23] Lozupone C, Knight R (2005) UniFrac: a new phylogenetic method for comparing microbial communities. *Appl Environ Microbiol* 71(12): 8228–8235.
- [24] McMurdie P-J, Holmes S (2013) phyloseq: an R package for reproducible interactive analysis and graphics of microbiome census data. *PLoS ONE* 8(4): e61217.
- [25] Oksanen J, Blanchet F-G, Kindt R, Legendre P, Minchin P-R, O'Hara R-B, *et al.* (2015) vegan: Community Ecology Package.
- [26] Anderson M-J (2001) A new method for non-parametric multivariate analysis of variance. *Austral Ecol* 26(1): 32–46.
- [27] Kembel S-W, Wu M, Eisen J-A, Green J-L (2012) Incorporating 16S gene copy number information improves estimates of microbial diversity and abundance. *PLoS Comput Biol* 8(10): e1002743.
- [28] Matsen F-A, Kodner R-B, Armbrust E-V (2010) pplacer: linear time maximum-likelihood and Bayesian phylogenetic placement of sequences onto a fixed reference tree. *BMC Bioinformatics* 11: 538.
- [29] Kembel S, Cowan P, Helmus M, Cornwell W, Morlon H, Ackerly D, *et al.* (2010) Picante: R tools for integrating phylogenies and ecology. *Bioinformatics* 26: 1463–1464.

- [30] Martiny A-C, Treseder K, Pusch G (2013) Phylogenetic conservatism of functional traits in microorganisms. *ISME J* 7(4): 830–838.
- [31] Jombart T, Dray S (2010) adephylo: exploratory analyses for the phylogenetic comparative method.. *Bioinformatics* 26: 1907–1909.
- [32] *Warning: citation key “altschul2990” is not in the bibliography database.*
- [33] Camacho C, Coulouris G, Avagyan V, Ma N, Papadopoulos J, Bealer K, *et al.* (2009) BLAST+: architecture and applications. *BMC Bioinformatics* 10: 421.
- [34] Yarza P, Richter M, Peplies J, Euzeby J, Amann R, Schleifer K-H, *et al.* (2008) The All-Species Living Tree project: a 16S rRNA-based phylogenetic tree of all sequenced type strains. *Syst Appl Microbiol* 31(4): 241–250.
- [35] Love M-I, Huber W, Anders S (2014) Moderated estimation of fold change and dispersion for RNA-seq data with DESeq2. *Genome Biol* 15(12): 550.